Journal of
Marine Science and Engineering

MDPI

Article

The Impact of Different Bow Shapes on Large Yacht Comfort

Ermina Begović [1,*], Enrico Della Valentina [2], Francesco Mauro [3,*], Radoslav Nabergoj [4] and Barbara Rinauro [1]

1 Department of Industrial Engineering, University of Naples Federico II, 80125 Naples, Italy
2 Maritime Research Institute Netherlands—MARIN, 6700 AA Wageningen, The Netherlands
3 Department of Maritime and Transport Technology, Faculty of Mechanical, Maritime and Materials Engineering, Delft University of Technology, Leegwaterstraat 17, 2628 CA Delft, The Netherlands
4 NASDIS PDS d.o.o., Industrijska Cesta, 2e, 6310 Izola, Slovenia
* Correspondence: e.begovic@unina.it (E.B.); f.mauro@tudelft.nl (F.M.)

Abstract: The importance of comfort during transfer and stationing becomes a key performance parameter for large yacht design, on the same level as propulsive issues. Such a matter extends questions in terms of form and service demand to the motion behaviour of the unit in waves. Relevant studies refer to outdated hull forms not specific to modern large yachts. In this study, five hull forms with different bow concepts represent the most common design solutions for yachts at constant draught and displacement. The preliminary ranking on the effect of alternative bows on comfort requires the definition of internationally accepted comfort standards. Here, the AWI 22834 guidelines for large yachts provide the service and environmental conditions and criteria for the comfort analysis, being the only reference specific to yachts. The calculations employ a strip-theory-based numerical model to provide results of easy understanding for designers during the early design stage. The obtained ranking among the design solutions on a reference large yacht favours the option nested with a bulb, contradicting the expectations in favour of a vertical bow concept. The discussion and conclusions provide a way forward for additional analyses and investigations aimed at proposing suitable multicriterial design guidelines for large yachts. However, the results also show the unsuitability of AWI environmental and encounter conditions for hull form ranking.

Keywords: hull forms; ship design; large yachts; comfort analysis; ship motions

Citation: Begović, E.; Della Valentina, E.; Mauro, F.; Nabergoj, R.; Rinauro, B. The Impact of Different Bow Shapes on Large Yacht Comfort. *J. Mar. Sci. Eng.* **2023**, *11*, 495. https://doi.org/10.3390/jmse11030495

Academic Editor: Vincenzo Crupi

Received: 31 January 2023
Revised: 15 February 2023
Accepted: 21 February 2023
Published: 24 February 2023

1. Introduction

In the past, in the preliminary design phase of a large yacht, calm water resistance minimisation was the main focus for hull form development. Recently the focus has extended towards seakeeping performances. In particular, comfort on board was a relevant topic in continuous expansion over the last decade, mainly for passenger ships, while large yachts present similar necessities. Any ship sailing at sea faces external forces due to wind, current and waves. These forces not only cause the ships' motions, which can reduce passengers' comfort, but are also responsible for increased resistance, continuous course adjustments, slamming phenomena and limitations in the operational profiles. Accelerations and motion minimisation are beneficial for the well-being of the crew and passengers. What remains challenging is obtaining a design with the desired level of motion and acceleration without compromising other ships' characteristics and performances.

The evaluation of vessels' comfort is a complex issue because it is subjective to human experiences and passengers' feedback can determine a vessel's reputation more than objective technical analysis. Until the 1980s, according to the literature [1], vertical accelerations were a prime measure of seasickness. Quantification of discomfort related to roll and transverse accelerations remained, apart from the impact on human mobility, out of reach. Such a matter was particularly disappointing because an onboard investigation [2] suggested that other acceleration components and motions played an important role, clearly indicating that roll and transverse accelerations were significant sources of human discomfort. Generally, motion-induced discomfort is related to three different aspects. The first source of seasickness regards the sensory conflict between the experienced accelerations and visual information. Several studies on human factors [3–10] have proposed illness ratings based on motion acceleration and frequency, exposure time, age and sickness history, i.e., whether people have previously been sick or not. A second aspect is the interference of the low-frequency horizontal and vertical accelerations with passenger activities and locomotion. The effect of ship motions on specific activities such as moving around on a ship or walking on a staircase may be bio-mechanical [11]. The last aspects relate to the coordination problems associated with high-frequency resonant phenomena in the human body leading to high sensitivity to vibration. These coordination problems may amplify the effects of low-frequency accelerations. Furthermore, almost all comfort criteria developed for operational and passenger ships cover almost only the cruising phase. However, for a large yacht, the design target is also to achieve an adequate comfort standard while stationing at anchor, which represents an important condition of their operational profile [12,13].

In recent years, the need for standardisation of comfort evaluation onboard large yachts in the early design stage led to the definition of a new standard specification for pleasure crafts: the AWI 22834 [14]. The specification proposes a set of typical environmental conditions and locations to assess comfort by evaluating characteristics related to vertical and lateral accelerations (a thorough description is given in Section 2.2).

All the mentioned studies conclude that ship motions are the dominant factor causing seasickness. It is also evident that, at constant displacement, longer vessels are more comfortable than smaller ones of similar configuration because the relative wavelength becomes shorter [15]. For this reason, the influence of principal dimensions on ship response in waves focuses on the effect of macroscopic changes in hull forms, especially for the forebody sections (U-shaped or V-shaped), and significant modifications in the hull form coefficients. The general indications suggest that a U-shaped forebody is advantageous for reducing speed loss, slamming occurrence and structural loads. V-shaped sections are beneficial for vertical motion reduction, especially for pitch motion.

More recent studies do not centre the focus on global hull form variations but are more oriented to the resolution of optimisation problems, considering only motions or multiple objective functions, including resistance [16–21]. The only exceptions concern the analysis of added resistance in waves [22,23] and the development of surrogate models for concept design using parametric analysis on coefficients [24,25]. However, these studies do not compare alternative concepts for the hull form or the forebody type.

The present paper's aim is to investigate the effect on the comfort of the most commonly adopted bow shapes for large yachts: conventional, bulbous and vertical. Such a topic is lacking in a proper investigation in the literature, as particular attention is given only to some specific designs without providing a valid comparison with alternative solutions. In fact, between classic and modern studies, the most relevant investigation on the influence of bulbous bows on ship motions is by Gerritsma and Beukelman [26], concluding that such an appendix does not substantially modify the ship's behaviour in waves. However, the study considers old hull forms and, given the phenomenon's complexity, it is not clear how different shapes of the modern bow affect the ship's motions in waves. Much confusion appears among the large yacht designers because a fair comparison among different modern bow shapes is missing in the literature for comfort, speed and course keeping. Therefore the current study is relevant to clarify the variations of comfort rating (based on the calculated accelerations) that can be expected by varying the shape of the bow or inserting a bulb.

Among the different possible bow configurations, the present work considers the three most adopted solutions for large yachts: conventional bow, conventional bow with bulb and vertical bow. The study compares, according to AWI-22834 standards, the comfort levels of five hulls generated from a reference 50 m yacht. Hull form variations concern only the forebody, maintaining the stern invariant. Modifications do not keep the displacement constant; therefore, two hulls have a different final draught to obtain the displaced volume of the original yacht. The analysis considers a fixed metacentric height GM of 1 m for all the hulls, resulting in different positions of the centre of gravity but keeping the radii of inertia constant.

The accelerations for the AWI-22834 conditions derive from 2D strip-theory calculations to adopt an analysis tool frequently used and understood by yacht designers. A critical discussion of the obtained results on a broader set of environmental conditions underlines the advantage of the vertical bow concept compared to other hulls, even though the results on AWI conditions favour the bulbous bow. However, the study suggests a more in-depth analysis of the hydrodynamic problem, considering non-linear effects and multi-attribute considerations, including resistance and course keeping, besides the pure comfort analysis.

2. Comfort Assessment on Large Yachts

In the design of a pleasure craft, comfort is of foremost importance. However, a unique and complete definition of comfort does not exist as it includes a subjective feeling by people. Moreover, the perception of comfort can be influenced by many factors, depending upon time to exposure, the intensity of the phenomenon, gender, age, previous experience and mental state of the subject. The following are the most relevant factors for large yachts:

- *Noise and vibrations*;
- *Motions and postural stability*;
- *Smell*;
- *On-board amenities, food and drink*;
- *Other factors* (weather, temperature, humidity, etc.).

The present study focuses on comfort due to wave-induced motions. Therefore, it is necessary to identify relevant criteria for motions/accelerations specific to large yachts, pinpointing pertinent thresholds to objectively judge the level of comfort or discomfort onboard. There are few examples in the open literature about motion/acceleration limits specific to pleasure crafts. Therefore, criteria dealing with vessel types close to yachts can provide general reference values. The following subsections provide an overview of general comfort criteria for passengers, compared with recently developed ones for large yachts, specifically.

2.1. General Comfort Criteria

General criteria for ship motion/acceleration limits exist in the literature and relate to different kinds of ships, ranging from operative offshore vessels to passenger ships, with plenty of dedicated criteria specific to naval ships [27,28].

Table 1 provides the general criteria applicable to passenger ships, even though they were intended for certain operations onboard naval vessels or operative ships. The activities and life onboard a yacht are more similar to passenger ships rather than navy activities; therefore, it is more reasonable to adopt criteria close to those used for passenger vessels. Unfortunately, specific criteria for passenger ships adopted inside MARIN [29] require the calculation of the Motion Illness Rating (MIR), which uses coefficients not available in the literature. Furthermore, its determination requires many parameters that would not be available in the early design stage.

General criteria may also apply to large yachts. However, standards for passenger ships refer to ships with larger sizes than yachts, thus providing potentially too restrictive thresholds for motion criteria. Searching for criteria specific to such vessels is then convenient for dealing with large yachts. The following section introduces AWI-22834 guidelines, proposing a framework for assessing comfort levels for such pleasure crafts.

Table 1. Comfort-related ship motion criteria applicable for passenger ships.

Criterion Name	Quantity	Criteria Fulfilment
Effective gravity angle	EGA	$RMS < 2$deg
ISO2631-1	MSI	$MSI < 10\%$
Comfort rating for passenger ships	MIR or CR	$MIR < 10$ (for passenger) $MIR < 20$ (for crew)
Nordforsk	Vertical acceleration Lateral acceleration roll	$RMS < 0.02g$ $RMS < 0.03g$ $RMS < 2$ deg
Vibration dose value	VDV	$VDV < 1$

2.2. AWI-22834 Guidelines for Large Yachts

As mentioned above, there is a lack of explicit standards and criteria specifically dedicated to large yachts. To this end, the ISO established the working group AWI-22834 [14], led by MARIN. The main goal of this working group is to produce a comparative scale of comfort among yachts to be used for technical and commercial benefits. The process goes through the definition and standardisation of the following points:

- Identification of yacht-specific comfort criteria;
- Environmental condition selection (wave height, period);
- Operative condition selection (vessel speed, encounter angle);
- Identification of onboard locations of interest;
- Evaluation of criteria satisfaction for all conditions.

Hereafter, individual sections describe the above-listed points included in the AWI guidelines.

2.2.1. Yacht Specific Comfort Criteria

As previously mentioned, available criteria for ship motion-related comfort (Table 1) refer to other vessel types, necessitating the identification of the most suitable comfort measures among available options. Among the available criteria, effective gravity angle (EGA) and Motion Sickness Index (MSI) are appropriate candidates for comfort assessment. The following formulation is suitable to describe EGA:

$$EGA = \arctan\left(\frac{\ddot{\eta}}{\ddot{\xi} + g}\right), \tag{1}$$

where g is the gravity acceleration and $\ddot{\xi}$ and $\ddot{\eta}$ are the absolute vertical and lateral acceleration, respectively. EGA calculation with Equation (1) is valid for each point of a vessel when evaluating accelerations for given points. Furthermore, Equation (1) is valid for both the time and frequency domains; in the latter case, it is necessary to use RMS values for absolute accelerations.

Concerning MSI, different formulations are available in the literature, with the following one selected as a reference for AWI calculations:

$$MSI = 100\Phi\left(Z_{\xi}\right)\Phi\left(Z_t'\right), \tag{2}$$

with relevant quantities in Equation (2) evaluated as follows [28]:

$$\Phi(Z) = \frac{1}{2\pi}\int_{-\infty}^{Z} e^{-\frac{x^2}{2}}\mathrm{d}x \text{ with } Z \in \left(Z_{\xi}, Z_t'\right), \tag{3}$$

$$Z_{\xi} = 2.128\log\left(\frac{\ddot{\xi}}{g}\right) - 9.277\log\hat{f}_{\xi} - 5.8099\log\hat{f}_{\xi}^{\,2} - 1851, \tag{4}$$

$$Z_t' = 1.134Z_{\xi} + 1.989\log T_e - 2.904, \tag{5}$$

where T_e is the exposure time in minutes and $\hat{f}_{\ddot{\xi}}$ is the frequency in Hertz of the absolute vertical acceleration $\ddot{\xi}$ spectrum peak. Therefore, Equation (2) is a simplified version of MSI, considering only the vertical acceleration. Such a choice allows a proper balance to be identified between the complexity of the criteria formulation and the need to have a sufficiently broad indicator to describe comfort. The combination between MSI and EGA covers, in the proposers' intentions, with a single extended index, the identification of passengers needing support (but also tipping or sliding of objects) and the percentage of people on board that will suffer from seasickness after a given exposure time.

2.2.2. Environmental and Operative Conditions

The AWI working group also proposes standard environmental conditions to assess comfort on large yachts. The selection of such conditions assumes that large pleasure vessels operate mostly in the Western Mediterranean and Caribbean Seas. Therefore, as a first simplified assumption, a combined wave scatter diagram of the two sea areas according to annual statistics identifies the reference environmental conditions for such yachts.

As an additional assumption, the analysis considers only the wave heights between 1 and 2 m: the waves with a higher occurrence in the combined scatter diagram, ensuring a fair compromise with at-anchor performances of vessels relatively short (less than about 60 m) and longer ones. Figure 1 shows an overview of the resulting environmental conditions. All the irregular wave conditions refer to long-crested sea approximation, modelled with a JONSWAP wave spectrum.

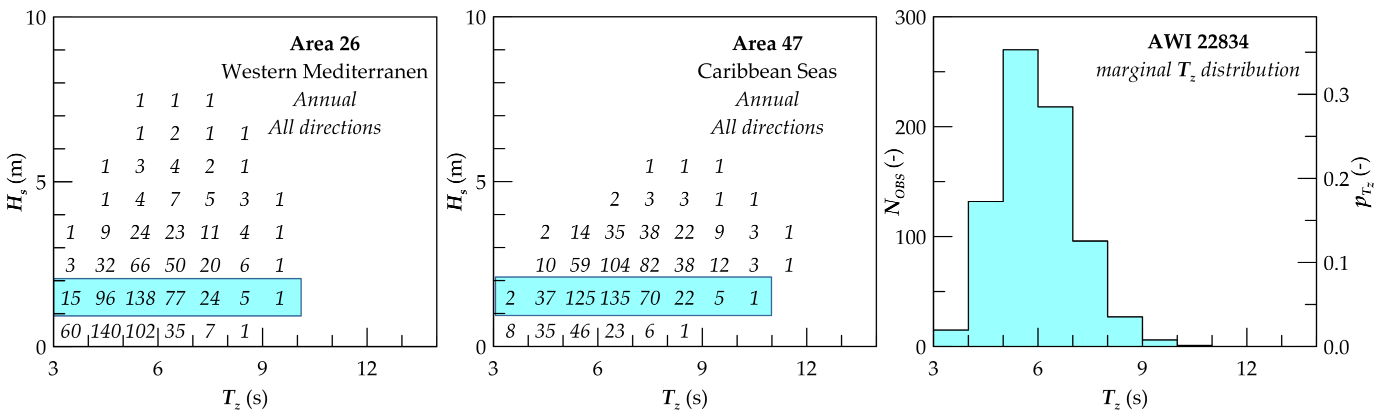

Figure 1. Environmental conditions considered by AWI 22834 guidelines.

Besides the environmental settings, additional simplifications concern the selection of the encounter wave conditions, which are determined by the course-keeping profile of the vessel. The analysis should be carried out for bow quartering seas over starboard only, analysing the mirrored position along the longitudinal axis for points not located on the yacht's diametral plane due to symmetry. The comfort analysis considers two reference speeds V: 0 and 12 knots. Such a choice covers the at-anchor condition and a general transfer one, recurrent in the large yacht operative profile.

2.2.3. On Board Location of Interest

According to the AWI proposers, the comfort analysis should consider five reference locations along the yacht, which are representative of five areas of interest for operations and leisure on board:

- Owner's cabin (OC)
- Dining area (DA)
- Wheel house (WH)
- Crew area (CA)
- Beach club (BC)

Each location mentioned above is represented by the geometrical centre of that space on board, adding 1.2 m to the reference deck height for the z coordinate, to represent the human centre of gravity. Therefore, the locations are not fixed for all the yachts but refer to individual general arrangements of the analysed units. However, according to the proposers, the selected reference areas are nowadays located in similar positions for large yachts, differing by small relative distances, which are not significant for large motion variations. Thus, the methodology is suitable for comparing alternative design solutions on the same platform or directly different vessels.

2.2.4. Comfort Satisfaction Thresholds

The last step necessary for the comfort assessment relates to defining the thresholds on the identified comfort criteria. The AWI proposers set, for all the environmental/encounter conditions, the fulfilment criteria to EGA < 2 deg and MSI < 10% with exposure time T_e equal to 1 h. Within this framework, it is then possible to identify the downtime period of the comfort criteria fulfilment at all speeds and locations as follows:

$$OP_C = \sum_{i=1}^{2} \sum_{j=1}^{N_L} \sum_{k=1}^{N_{T_z}} p_{V_i} p_{L_j} p_{T_{z_k}} I_{C_{ijk}}, \tag{6}$$

where p_V and p_L are the weighting functions for speeds and onboard locations, while p_{T_z} is the marginal distribution of the wave periods described in previous subsections. The preliminary AWI proposal considers an equal weight within the five locations and the two speeds, resulting in p_L = 0.2 and p_V = 0.5, respectively. For all the conditions, the functional I_C [30] identifies whether the comfort criteria are above or under the suggested thresholds:

$$I_C = \begin{cases} 1 & \text{if } MSI < 10\% \vee EGA < 2\,\text{deg}, \\ 0 & \text{otherwise.} \end{cases} \tag{7}$$

As an outcome of the comfort analysis, the AWI guidelines propose a rating ranking based on the values of OP_C according to a five star scale. Table 2 reports the rating system, which can be global or local: in the latter case, it is sufficient to neglect the loop on locations or speeds from Equation (6).

Table 2. AWI 22834 rating system.

OP_C (%)	Star Rating	Qualitative Rating
0–20	★☆☆☆☆	Poor
20–40	★★☆☆☆	Below average
40–60	★★★☆☆	Average
60–80	★★★★☆	Good
80–100	★★★★★	Very good

3. Large Yacht Hull Concepts

The bow shape design of a large yacht necessitates the combined satisfaction of hydrodynamic and aesthetic issues. The first is necessary to grant vessel performances, while the second is related to the harmonic combination between the hull and the superstructures. There are multiple possibilities for the bow shape selection; however, there is a lack of general indications about the advantages and disadvantages of alternative solutions for motion reduction and comfort.

In recent years, some new solutions for bow shapes also appeared in the yacht market, like the wave piercer bow or the inverse rake bow. Nonetheless, these applications remain restricted to a few unique applications in the pleasure craft market. Consequently, the most commonly adopted solutions for yachts remain the following ones:

- Conventional bow;
- Conventional bow with bulb;

- Vertical bow.

The following sections describe the three bow design options and introduce the hull forms analysed in the present work.

3.1. Conventional Bow

The conventional bow concept (see Figure 2) is the most diffused bow type in the yacht industry, especially for units shorter than 50 metres. This choice is probably a consequence of the reduced construction costs and the almost standard superstructure layout well fitted by a clipper bow. Especially for small units, the hydrodynamic issues mainly related to calm water resistance and propulsion favour the adoption of such a bow type, as the associated Froude number regimes for the transfer and full speed conditions can be above 0.3–0.4, thus appropriate for a conventional bow.

Figure 2. Conventional bow example.

Conventional bows for yachts imply that the fore sections of the hull present a large flare, resulting in a high susceptibility to impact with incoming waves in transit and anchor conditions. Hence, it is highly probable that phenomena associated with wave-induced vibration, such as comfort, are present with consistent relevance. Figure 2 shows the typical shape of the forebody of yachts fitted with this bow concept, highlighting the presence of the pronounced flare. Such a bow concept is also typical of fast yachts sailing in half-planing or planing conditions. For these conditions, the bow may also present the spray rails, sometimes fitted likewise on fast displacement yachts to reduce the bow flare, as highlighted in Figure 3.

Figure 3. Conventional bow example with spray rail.

3.2. Conventional Bow with Bulb

Besides the conventional bow, the widely diffused forebody typology for large yachts is the bulbous bow (see Figure 4). Such a solution is particularly effective for vessels sailing in a Froude number range between 0.2 and 0.3, where the bulb grants a relevant abatement of wave-making resistance [31–33]. As the transfer/cruise speed of large yachts is almost invariant with the vessel dimensions, the bulbous bow solution is more suitable for medium/long units instead of small ones. However, the confusion and lack of general guidelines in the literature make it typical practice for some yacht designers to fit bulbous bows outside the optimum range of Froude numbers, especially for retrofitting an old yacht. Such a mistake is associated with the expectation of obtaining a wave-making resistance reduction compared to the original hull, regardless of hydrodynamic analyses.

Figure 4. Conventional bow with bulb example.

Figure 5 shows the nesting of a bulbous bow during the retrofitting of an old vessel with a conventional bow type. The Figure shows that adding a bulb in the forebody does not change the above waterline characteristics of the sections. Therefore, in the case of a bulb-fitted conventional bow, the same issues concerning the flare will appear. At the same time, the bulb can be nested into all the kinds of bows applicable to a vessel, supposing that the design conditions are suitable for the beneficial effects provided by the bulb.

Figure 5. Nesting of a bulb on an existing yacht with conventional bow.

The form and dimensions of the bulb should result from a careful hydrodynamic study based on the yacht operative profile and the constraints provided by the ship owner; otherwise, the fitting of such an appendix cannot produce the desired performance improvements.

3.3. Vertical Bow

Another bow shape rising in popularity in the last ten years is the vertical bow (see Figure 6). The main characteristic of this forebody type is the absence of a longitudinal difference between the waterline and the main deck termination in the forebody. As a result, by keeping the same workable area on the main deck, the vessel with the vertical bow has a longer waterline length than units provided with a conventional bow.

Figure 6. Vertical bow example.

However, the calm-water wave-making resistance reduction is not the only benefit achievable with a vertical bow. The forebody shape drastically changes compared to conventional hull forms, especially the forebody sections above the waterline. In the case of a vertical bow, the bow sections do not present the characteristic flare of the conventional bow type. The main reason is the slight difference in the offsets between the waterline and the main deck, resulting in more straight and V-shaped sections. Such behaviour is visible in Figure 6. The direct consequence of fitting a V-shaped section in the forebody is decreasing the bow flare. Therefore, it is expectable that all phenomena associated with the impact between the hull and incoming waves at zero or transit/cruise speed will decrease compared to a conventional bow. Hence, the vertical bow can be beneficial to increase the comfort onboard large yachts, even though there are no guidelines to quantify the benefit in an early design stage. Furthermore, adopting a vertical bow does not prevent the fitting of additional appendages like a bulb or the spray rails already discussed for the conventional bow type.

The advantages of a vertical bow make this forebody type the starting point for developing different bow shapes, like the axe bow or the reverse bow. However, the diffusion of such new bow types in the large yacht market is limited and less relevant than the vertical bow.

3.4. Reference Hull Forms

The hulls selected for the comparison derive from a representative displacement hull form (large motor yacht). From this initial form, only variations of the bow shape lead to the definition of two new hulls for investigating the effect of the bow shape on the accelerations of the rigid body. The reference hull (hereafter called Hull A) is a displacement hull form of a Motor Yacht with a traditional bow shape and flare without the bulbous bow, tested at MARIN in 2014 [34]. The adopted initial geometry does not reproduce the final yacht hull because of confidentiality agreements between MARIN and customers. Two other hulls were generated, starting from Hull A, changing only the bow shape and keeping the draught constant. Hull B is a variation obtained by inserting a bulb, while Hull C presents a vertical bow. The three hulls have the same shape from the midship section to the extreme stern; furthermore, Hull B has the same hull shape except for the insertion of the bulb. Figure 7 shows the side view of the three described hull forms, while Figure 8 shows the sections of the hulls.

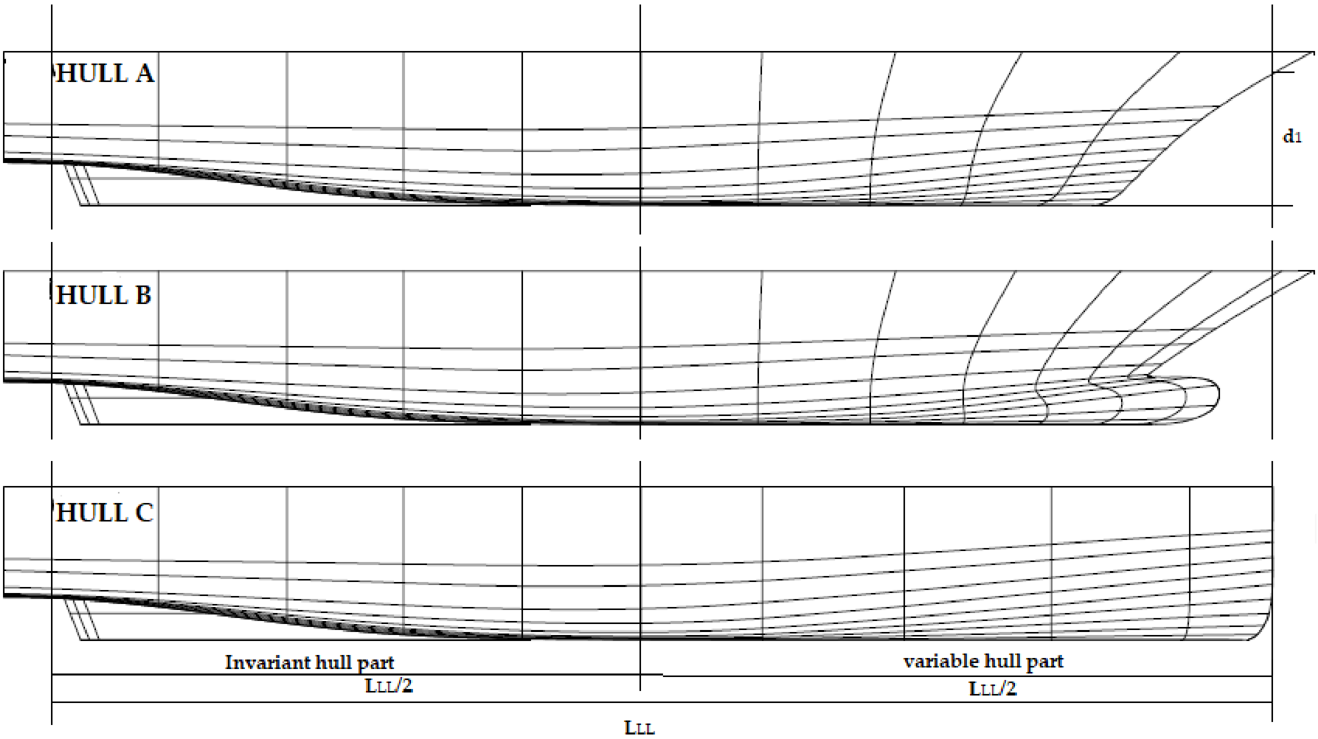

Figure 7. Side view of the hull forms considered in the study with conventional (Hull A), bulbous (Hull B) and vertical bow (Hull C), respectively.

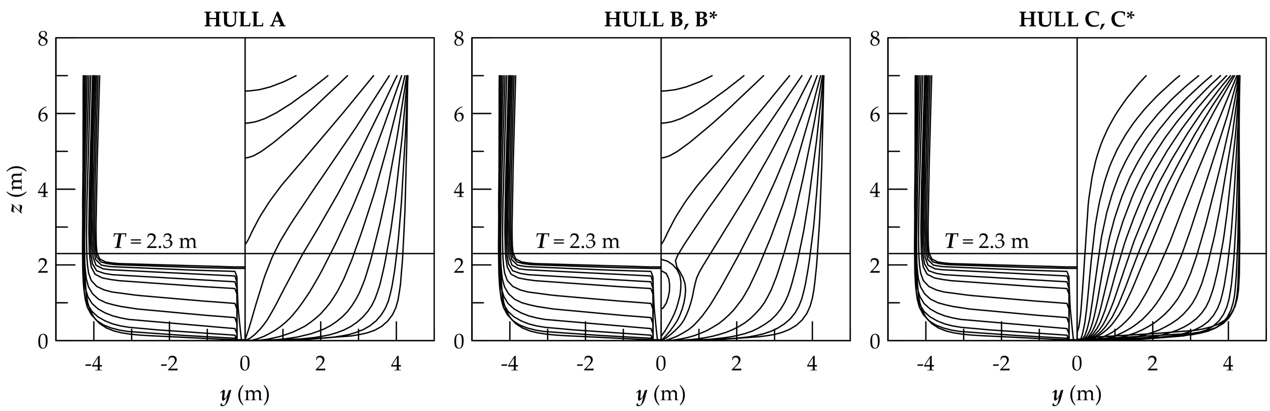

Figure 8. Sections of the hull forms considered in the study with conventional (Hull A), bulbous (Hull B) and vertical bow (Hull C), respectively.

The main goal of this selection is to make a fair comparison among the bows from a designer's point of view while assisting a potential customer in selecting the most suitable bow shape for their yacht. In this sense, it is necessary to adopt a nomenclature familiar to both designers and shipowners, employing the load line length L_{LL} as a reference and maintaining it invariant for each hull while keeping the volume ∇_{LL} constant under this line. The L_{LL} is a fictitious length measured on the waterline at a draught d_1 corresponding to 85% of the construction height D, keeping the longer value between 96% of the waterline or the distance between the fore waterline point and the axis of the stock rudder [35]. Such an approach for flat keel hulls is presented in Figure 9. Nevertheless, as a consequence of the load line length concept, the length between perpendiculars L_{PP} and the displacements Δ are not the same for the three hulls.

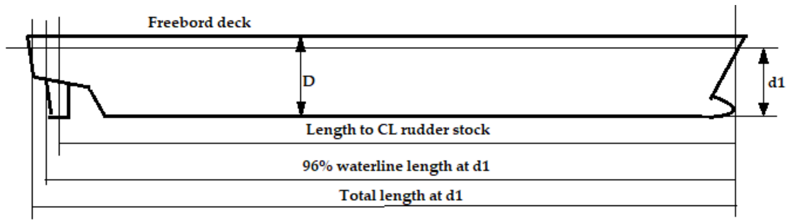

Figure 9. Load line length determination for flat keel hulls.

However, the displaced mass in salt water Δ is a fundamental attribute for ship design, influencing the inertial matrix of the ship, the longitudinal position of the centre of gravity x_G for even keel conditions and, consequently, seakeeping characteristics. Therefore, this study considers two additional hulls (namely Hull B* and C*) for the comfort analyses directly derived from Hull B and Hull C. The variations consist of a change of draught T necessary to match the saltwater displacement of Hull A; thus, the two hull forms do not need additional visualisation as the sectional shape remains the same.

Furthermore, the five hulls also differ in other hull-form parameters and the centre of gravity position. The longitudinal position x_G is taken equal to the centre of buoyancy x_B to have a static even-keel condition. The vertical position z_G ensures a value of the metacentric height GM of 1 metre invariant for each hull. Such a choice is necessary to maintain a fair comparison between the shapes of the bows, without introducing additional inertial effects. The adopted GM value is coming from statistical assumptions derived from previous studies at MARIN [34]. Table 3 reports the main characteristics of the five hulls, derived from the hulls' hydrostatics (for Hull B* and C* the values refer to Hull B and C at the draught corresponding to Hull A displacement).

Table 3. Reference hulls' main characteristics.

Characteristic	Symbol	Unit	HULL A	HULL B	HULL C	HULL B*	HULL C*
Length between perpendiculars	L_{PP}	m	50.000	50.000	52.292	50.000	50.000
Waterline length	L_{WL}	m	52.798	52.798	57.942	53.842	57.942
Load line length	L_{LL}	m	55.650	55.650	55.650	55.650	55.650
Maximum breadth at design draught	B_{max}	m	8.602	8.602	8.602	8.597	8.595
Design draught	T	m	2.300	2.300	2.300	2.285	2.229
Displacement mass in seawater	Δ	t	585.2	593.9	616.3	585.2	585.2
Longitudinal position of the centre of gravity *	x_G	m	23.693	24.037	24.881	26.221	24.950
Vertical position of the centre of gravity *	z_G	m	3.586	3.603	3.530	3.643	3.639
Metacentric height	GM	m	1.000	1.000	1.000	1.000	1.000
Natural roll period	T_ϕ	s	7.320	7.410	7.420	7.34	7.350

* Measures are given taking the intersection between the aft perpendicular and the keel line as origin.

4. Hull Concept Comfort-Rankings Results

The comparison between the five different hulls follows, as mentioned earlier, the AWI guidelines for comfort on large yachts. Even though the guidelines indicate the environmental conditions, comfort criteria and subsequent comfort rating, no specific restriction applies to the source of accelerations needed to evaluate comfort onboard.

This work concerns a preliminary design stage; hence, the investigation adopts accelerations derived from 2D strip-theory calculations with all the associated assumptions and limitations. This section briefly describes the numerical model used to calculate the accelerations, defines the location of interest for the five hulls and concludes with the final ranking among the different hulls.

4.1. Numerical Model

The well-known 2D strip theory is a suitable option, accessible to designers, to perform fast seakeeping calculations during an early design stage. Here, the 2D code SHIPMO [36] allows the hydrodynamic forces to be determined and the motion equations to be solved. A 2D strip theory implies a set of assumptions and limitations to the calculations, such as the linearity of the body forces and the validity for small amplitude motions, supposing that the hull has theoretically vertical sides.

As usual in strip theory, the hull form is approximated by an arbitrary number of sections composed of line elements without direct hydrodynamic interaction between the strips. In the present study, 21 strips define Hulls A, C and C*, and 24 strips Hulls B and B*. All sections include 50 to 100 line elements, modelling both vessel sides. SHIPMO solves the fundamental radiation–diffraction problem for each strip, calculating the corresponding hydrodynamic forces. After evaluating the wave excitation and the reaction forces on the individual sections, the global forces result from integration over the ship length. The determination of excitation (Froude–Krylov and diffraction) and reaction forces (added mass and damping coefficients) allows motion equations to be solved, including nonlinear effects like viscous roll damping due to eddies around bilge, skin friction damping, lift damping, presence of bilge keels, skegs and rudders, passive and active fins or anti-roll tanks. The numerical model of the five hulls does not consider appendages such as bilge keels, stabiliser fins, and bow and stern thruster tunnels. Only two rudders contribute to the roll damping coefficient, evaluated with the Ikeda method [37].

Despite the theoretical limits of linear strip theory, the SHIPMO program covers a wide range of applications and hull forms, being suitable for an initial comparison between different hull forms. As the AWI environmental conditions do not require motion prediction in extreme conditions, theoretical limits of the code are acceptable for the present study. In any case, a detailed description of the numerical methods, code validations and limitations is present in the literature [38].

The execution of SHIPMO calculations on the five reference hull forms allows the barycentric motions' relative amplitude operators (RAOs) to be determined for the AWI conditions (heading and speed). Figures 10 and 11 show the 6 degrees of freedom barycentric RAOs for 0 and 12 knots, respectively. RAOs refer to the AWI reference heading of 135 degrees, according to the adopted reference system (see Figure 12). Calculations refer to a frequency range between 0 and 7 rad/s, but, for representation purposes, the figures report only the scope between 0.5 and 3.0 rad/s. The barycentric radii of gyrations of the five hulls refer to the following standard values suitable for large yachts:

$$k_{xx} = 0.37 B_{max}, \tag{8}$$

$$k_{yy} = 0.25 L_{WL}, \tag{9}$$

$$k_{zz} = 0.25 L_{WL}. \tag{10}$$

The k_{yy} and k_{zz} are consequently different for all the hulls, according to the L_{WL} values reported in Table 3. Such values for the radii of gyrations derive from analyses performed by MARIN on an internal reference model test database [34].

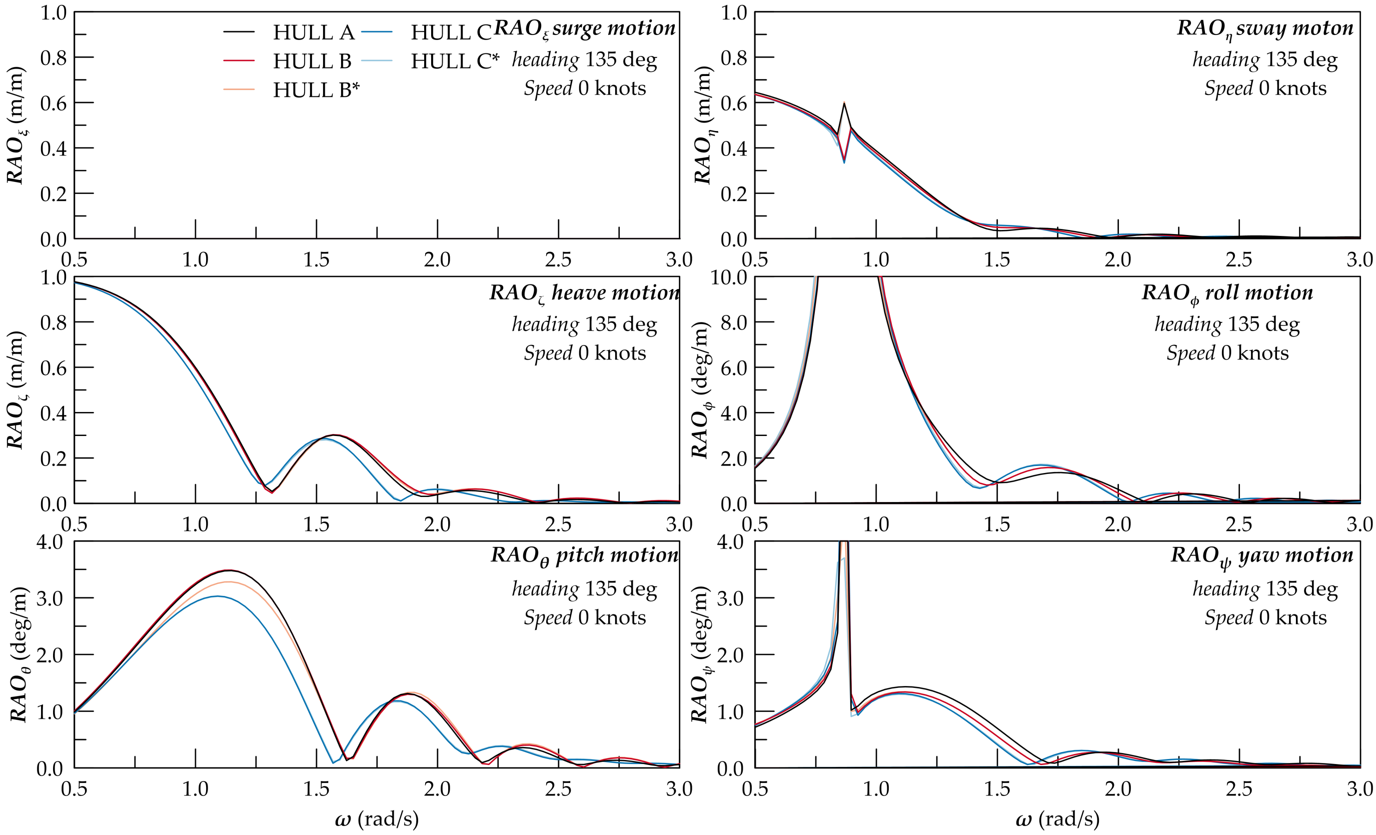

Figure 10. Six DOF RAOs at 0 knots on the reference hulls for the AWI heading of 135 degrees.

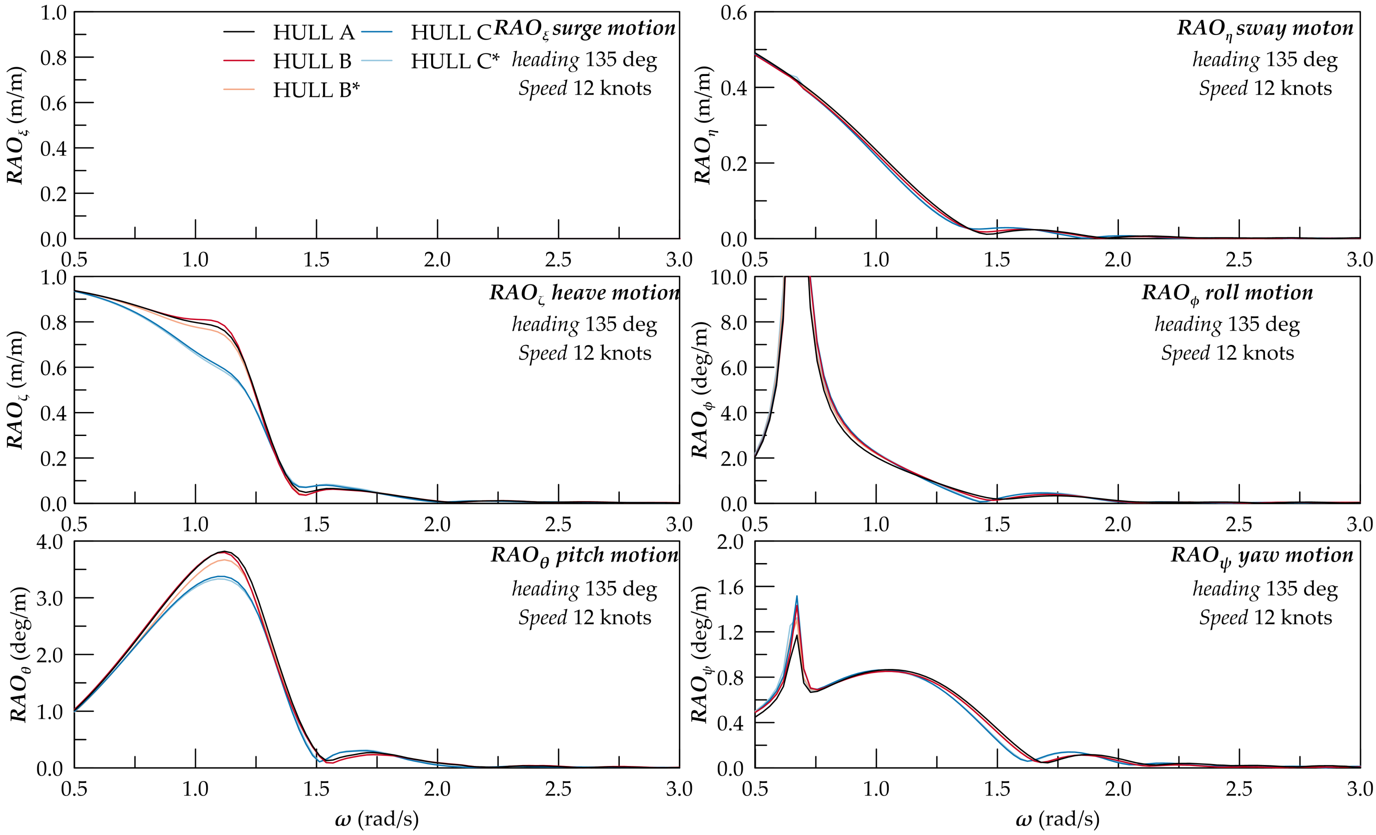

Figure 11. Six DOF RAOs at 12 knots on the reference hulls for the AWI heading of 135 degrees.

Few differences appear, analysing the obtained curves, in the barycentric RAOs between Hull A and Hull B, highlighting the same trends observed by Gerritsma in their studies on the addition of a bulb [26]. Hull C presents more differences from the original hull form, especially for heave and pitch motions. Even though hulls A, B and C have different displacements, analogue considerations pertain to hull versions B* and C*. Hull C* presents barycentric RAOs comparable with Hull C for all the six DOFs. For hull B*, little difference appears in pitch motion amplitude around 1.0 rad/s compared to Hull B. Therefore, an analysis based on barycentric RAOs only suggests that Hull C and C* are less susceptible to vertical motions than Hulls A and B. However, there being differences in the positions of the centre of gravity between the five hulls, it is necessary to consider the absolute motions/accelerations in the specific locations suggested by AWI guidelines.

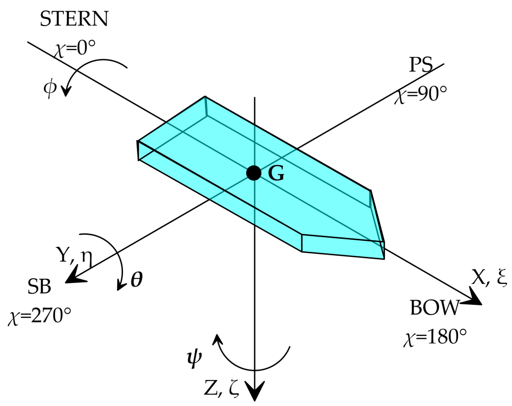

Figure 12. Reference system adopted for the seakeeping calculations.

4.2. Locations

The application of AWI 22834 guidelines requires the evaluation of MSI and EGA in five specific locations along the yacht, according to the formulations given by Equations (2) and (1), respectively. Such equations require knowledge of the vertical and lateral accelerations characteristic of the points indicated by AWI 22834 (see Section 2.2). Table 4 reports the coordinates of the locations at which AWI 22834 guidelines require the execution of the comfort analysis.

Table 4. Coordinates of the AWI 22834 locations on the reference hulls *.

Location	Symbol	x_L (m)	y_L (m)	z_L (m)
Owner's cabin	OC	41.712	0.000	7.500
Dining area	DA	21.700	0.000	5.850
Wheel house	WH	36.498	−2.000	9.170
Crew area	CA	45.188	0.000	2.500
Beach club	BC	3.134	0.000	4.170

* Measures are given taking the intersection between the aft perpendicular and the keel line as origin.

Motions and accelerations at specific locations along the vessel require barycentric values. For the analysed cases in vertical and lateral directions, the transformation equations are as follows:

$$\eta_L = \eta_G - \frac{2\pi}{\lambda}[\theta(z_L - z_G) + \psi(x_L - x_G)], \quad (11)$$

$$\zeta_L = \zeta_G - \frac{2\pi}{\lambda}[\theta(x_L - x_G) + \phi(y_L - y_G)], \quad (12)$$

where subscript $_G$ denotes the centre of gravity and $_L$ the generic location along the hull. Equations (12) and (11) are valid for frequency and time domain simulations. As the analysis is performed in the frequency domain, the two equations transform the barycentric values into local RAOs, obtaining the acceleration RAOs from the motion by multiplying by the encounter frequency ω_e:

$$RAO_{\ddot{\eta}_L} = RAO_{\eta_L}\omega_e^2, \tag{13}$$
$$RAO_{\ddot{\zeta}_L} = RAO_{\zeta_L}\omega_e^2. \tag{14}$$

The resulting local absolute lateral and vertical acceleration RAOs will have more distinctions between the five reference hull forms compared to the barycentric responses shown in the previous section. The different positions of the centre of gravity between the reference hulls should provide different arms in transformation Equations (11) and (12), thus increasing the differences in the resulting local RAOs. Figures 13 and 14 show the lateral acceleration RAOs for the AWI locations and heading for the speeds of 0 and 12 knots, respectively. The local RAOs have more variability compared to the barycentric ones, especially for locations far away from the centre of gravity. This is true for both 0 and 12 knots and confirmed by the fact that the dining area (DA), which is the closest location to the centre of gravity, shows few differences between the five hull forms.

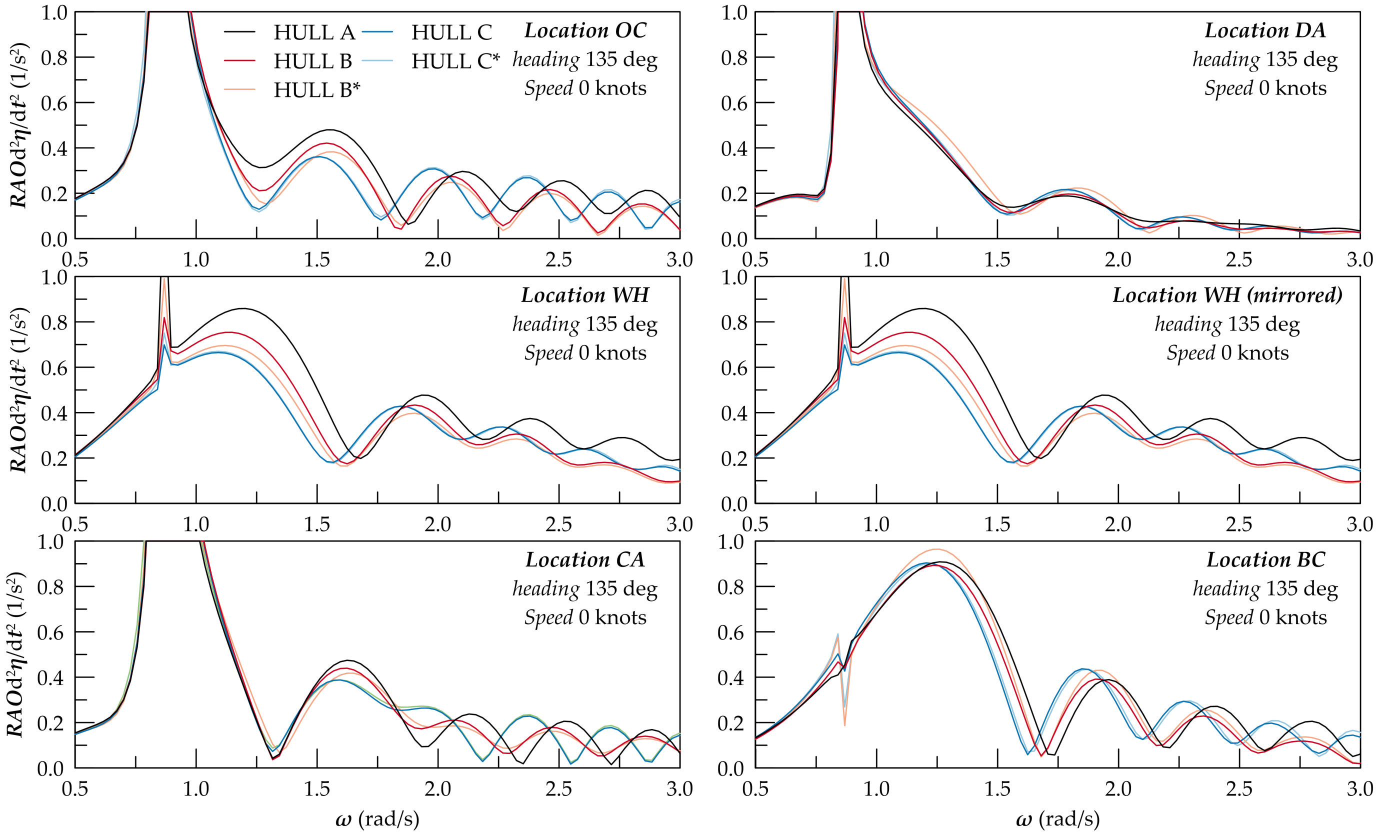

Figure 13. Absolute lateral acceleration RAO at 0 knots on the reference hulls for the AWI locations.

Figures 15 and 16 show the vertical acceleration RAOs for the AWI locations and heading for the speeds of 0 and 12 knots, respectively. The same considerations made for the lateral accelerations pertain to the vertical ones. Furthermore, in this case the variability between the five hull forms is higher for locations away from the centre of gravity at both vessel speeds. From the local RAOs calculated on the five hull forms, the vertical and lateral amplitudes observed for Hull C and C* are lower than the other design solutions for the 0 speed. At 12 knots, Hull B* also shows low acceleration amplitudes, which are comparable with Hull C and C*. However, a pure comparison and ranking on the local absolute acceleration RAOs is not sufficient to judge the final comfort levels of the five hull forms. Therefore, a frequency domain analysis is needed for the AWI 22834 conditions.

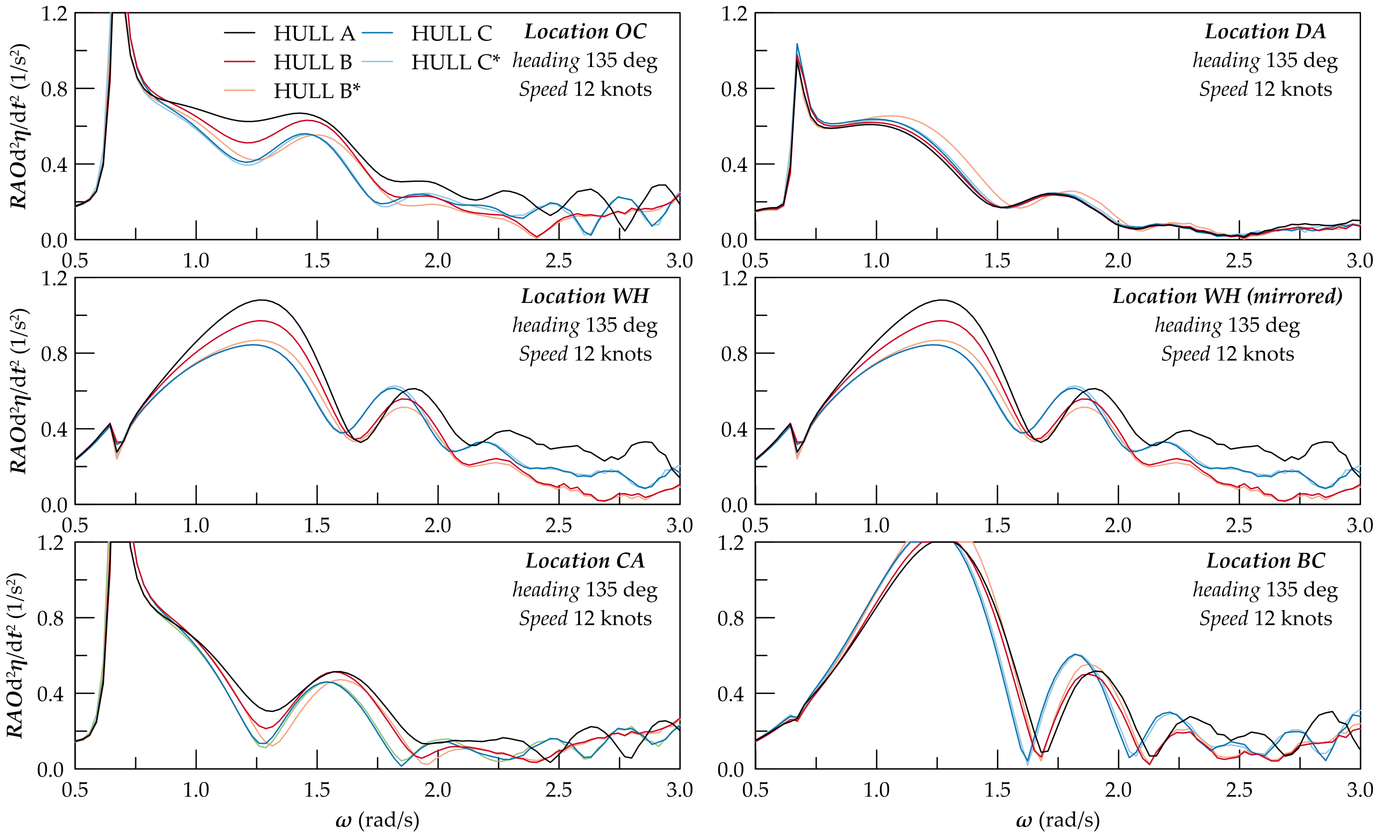

Figure 14. Absolute lateral acceleration RAO at 12 knots on the reference hulls for the AWI locations.

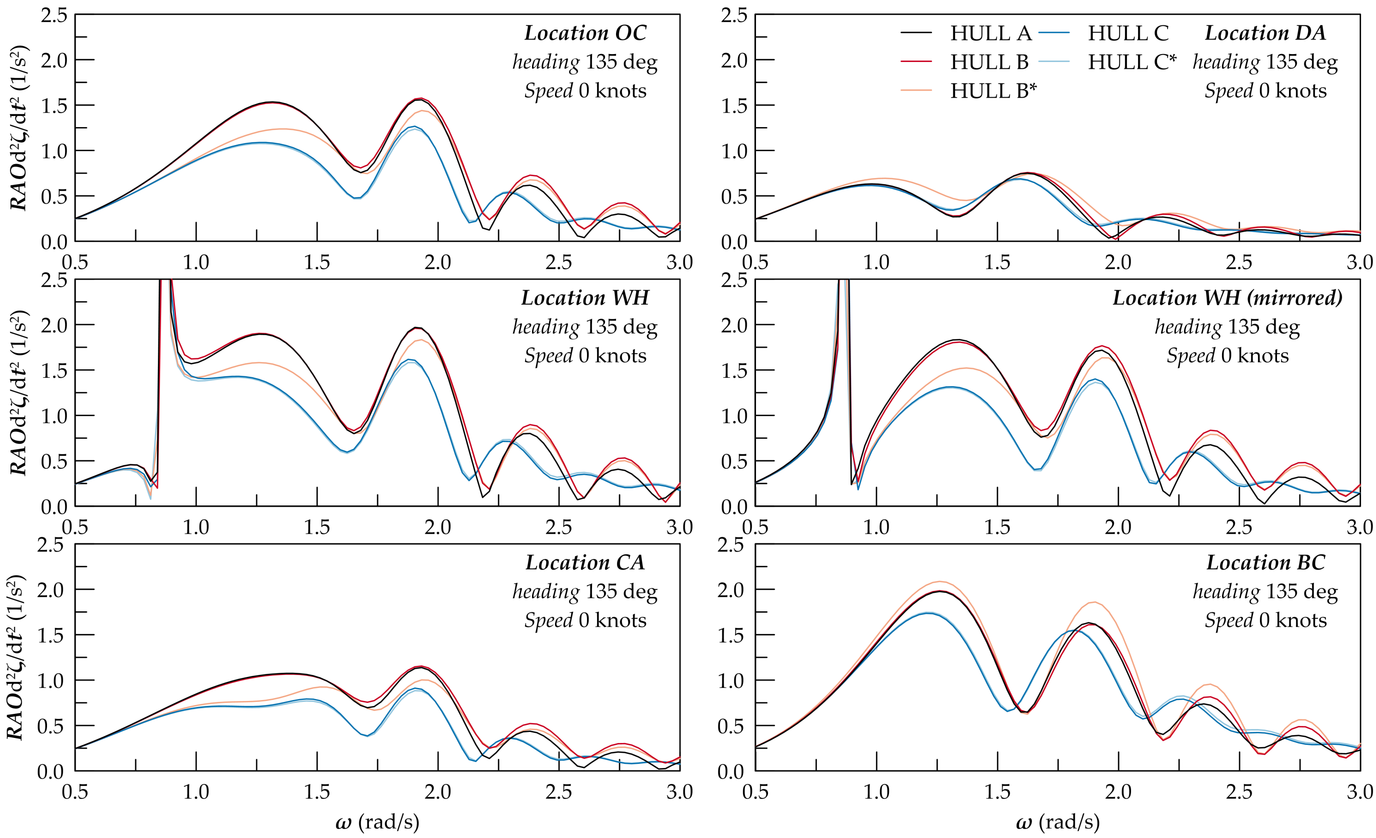

Figure 15. Absolute vertical acceleration RAO at 0 knots on the five reference hulls for the AWI locations.

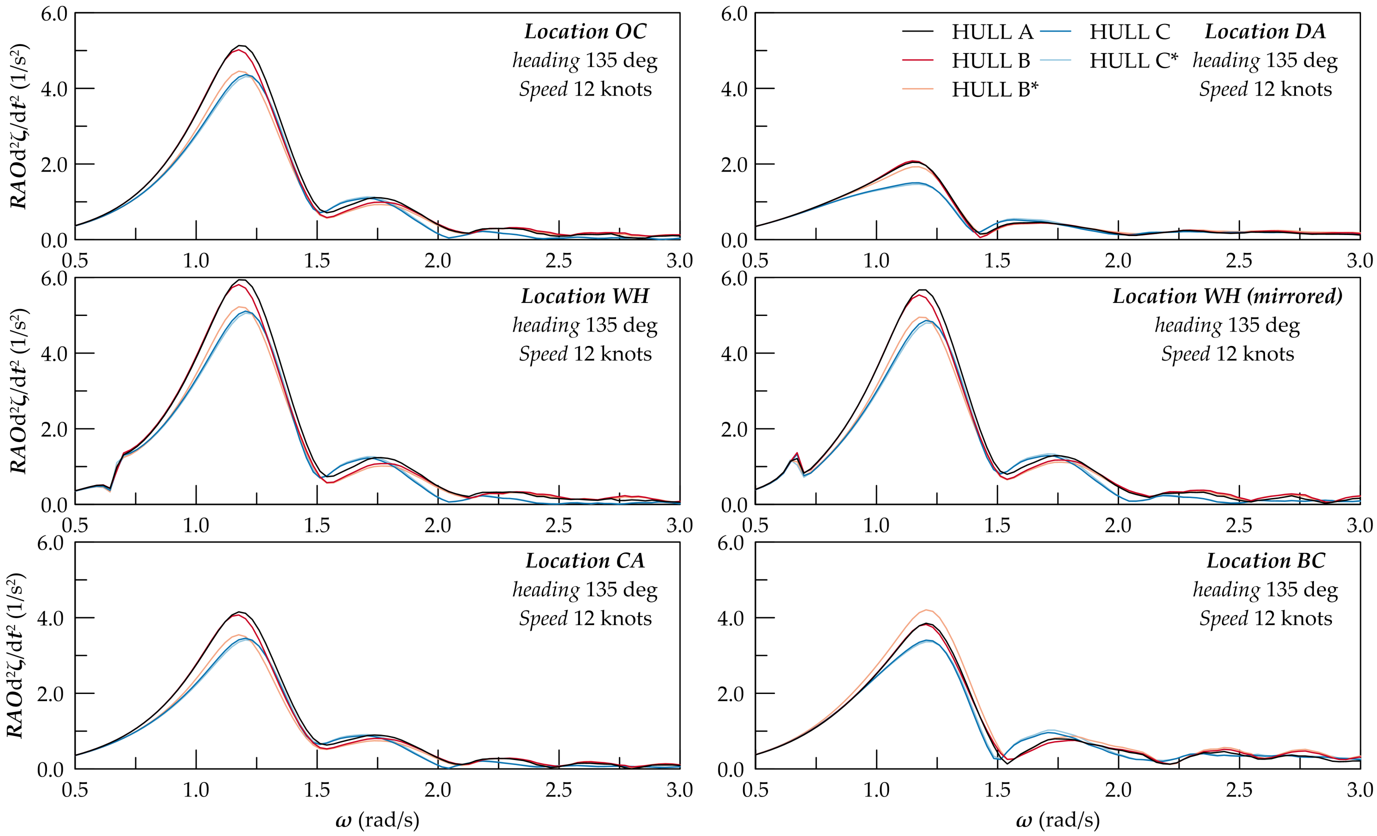

Figure 16. Absolute vertical acceleration RAO at 12 knots on the five reference hulls for the AWI locations.

In a frequency domain calculation the final MSI and EGA values are calculated on a base of $\ddot{\eta}$ and $\ddot{\zeta}$ RMS values, and, in the case of MSI, using additional characteristics of the vertical acceleration spectrum $S_{\ddot{\zeta}_L}$ (see Equation (2)). The acceleration spectra consider the environmental conditions suggested by AWI 22834 guidelines concerning H_s and T_z, corresponding to the scatter diagram cells highlighted in Figure 1. The guidelines suggest the adoption of a JONSWAP-like spectrum. Usually, the well known elongation parameter γ of the JONSWAP spectrum is 3.3 but there is the possibility to use different γ values as a function of the wave period T_z [39,40]. The present study employs the second option, leading to the wave spectra in Figure 17 for the comfort calculations. Such wave amplitude spectra derive from the following definition of the JONSWAP spectrum:

$$S_W = A(\gamma) S_{W_0} \gamma^{\exp\left[-\frac{1}{2}\left(\frac{\omega-\omega_p}{\sigma\omega_p}\right)^2\right]}, \tag{15}$$

where:

$$S_{W_0} = \frac{5}{16} H_s^2 \omega_p^4 \omega^{-5} \exp\left[-\frac{5}{4}\left(\frac{\omega}{\omega_p}\right)^{-4}\right], \tag{16}$$

$$\gamma = \begin{cases} 1 & \text{for } T_p/H_s^{0.5} \geq 5, \\ \exp\left(5.75 - 1.15 T_p/H_s^{0.5}\right) & \text{for } 3.6 < T_p/H_s^{0.5} < 5, \\ 5 & \text{for } T_p/H_s^{0.5} \leq 3.6, \end{cases} \tag{17}$$

$$\sigma = \begin{cases} 0.07 & \text{for } \omega \leq \omega_p, \\ 0.09 & \text{for } \omega > \omega_p, \end{cases} \tag{18}$$

$$A(\gamma) = 1 - 0.287 \ln \gamma, \tag{19}$$

$$T_p = 0.6673 + 0.05037\gamma - 0.00623\gamma^2 + 0.0003341\gamma^3. \tag{20}$$

In the above equations, ω_p is the peak frequency and S_{W_0} is the Pierson–Moskowitz spectral formulation. For the AWI conditions shown in Figure 17 all the periods above 4 s present $\gamma = 1$, thus irregular sea-states described by a Pierson–Moskowitz spectrum (fully developed sea). Only for $T_z = 3.5$ s is the enhancement parameter higher, representing a growing sea environment. In any case, all tested conditions refer to a long-crested sea model.

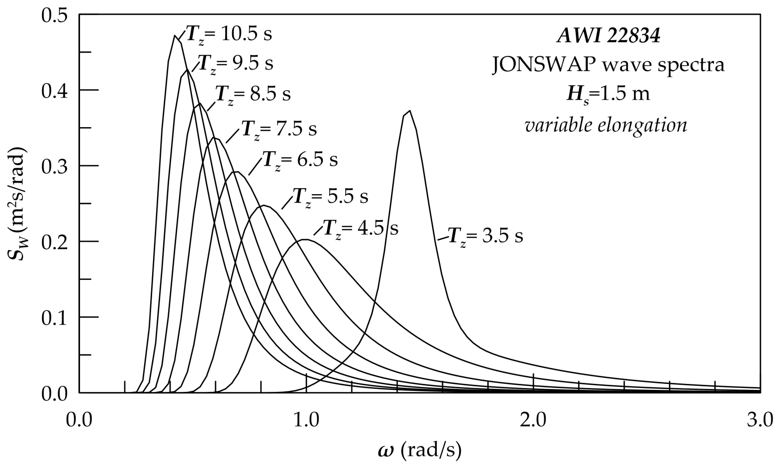

Figure 17. JONSWAP wave spectra for AWI environmental conditions.

Having defined the wave spectra it is possible to evaluate the vertical and lateral acceleration spectra for the specific AWI 22834 conditions, coupling the absolute local RAOs with the associated wave environment spectrum S_W:

$$S_{\ddot{\eta}_L} = S_W \, RAO^2_{\ddot{\eta}_L}, \tag{21}$$

$$S_{\ddot{\zeta}_L} = S_W \, RAO^2_{\ddot{\zeta}_L}. \tag{22}$$

Equation (21) allows the RMS value of the absolute lateral acceleration for the AWI locations to be determined, given by the square root of the spectral area, necessary to determine the EGA according to Equation (1). Equation (22) provides the spectrum of the vertical acceleration that should be processed to derive the frequency $\hat{f}_{\ddot{\zeta}}$ at which the maximum amplitude of $S_{\ddot{\zeta}_L}$ is necessary for the MSI evaluation. Integrating the spectra allows also the evaluation of RMS values for vertical absolute local accelerations, needed to compute EGA and MSI.

The application of Equations (1) and (2) with RMS values of local vertical and lateral absolute accelerations allows the AWI 22834 comfort criteria to be checked in the five prescribed locations. Figures 18 and 19 show the EGA values obtained for $H_s = 1.5$ metres and a varying T_z between 1 and 15 s for 0 and 12 knots and heading 135 degrees, thus for operative conditions including the AWI suggested ones. The figures also represent the AWI threshold of 2 degrees for the EGA value. Analysing the 0 knots condition (Figure 18), it can be observed that the AWI threshold is exceeded only for the owner's cabin (OC), the dining area (DA) and the crew area (CA) locations. All the hull forms exceed the limit; however, the T_z range of exceedance changes hull by hull. For all the locations, Hull C* presents a thinner exceedance range among the tested forms. The situation is different for 12 knots (see Figure 19), where the AWI threshold is exceeded in the crew area (CA) only, but not by hull forms A and B*.

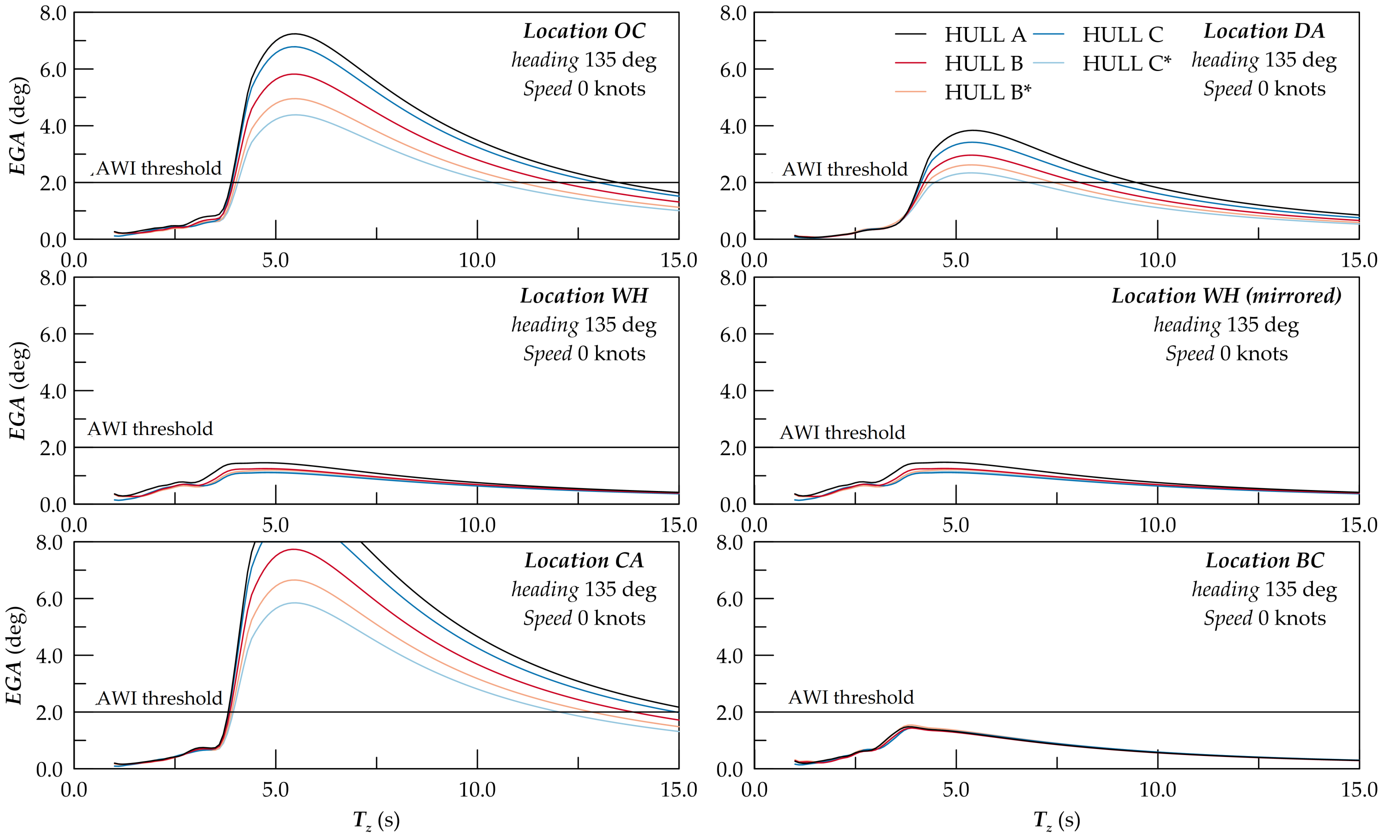

Figure 18. EGA values for $H_s = 1.5$ metres at different T_z for the AWI 22834 locations at 0 knots.

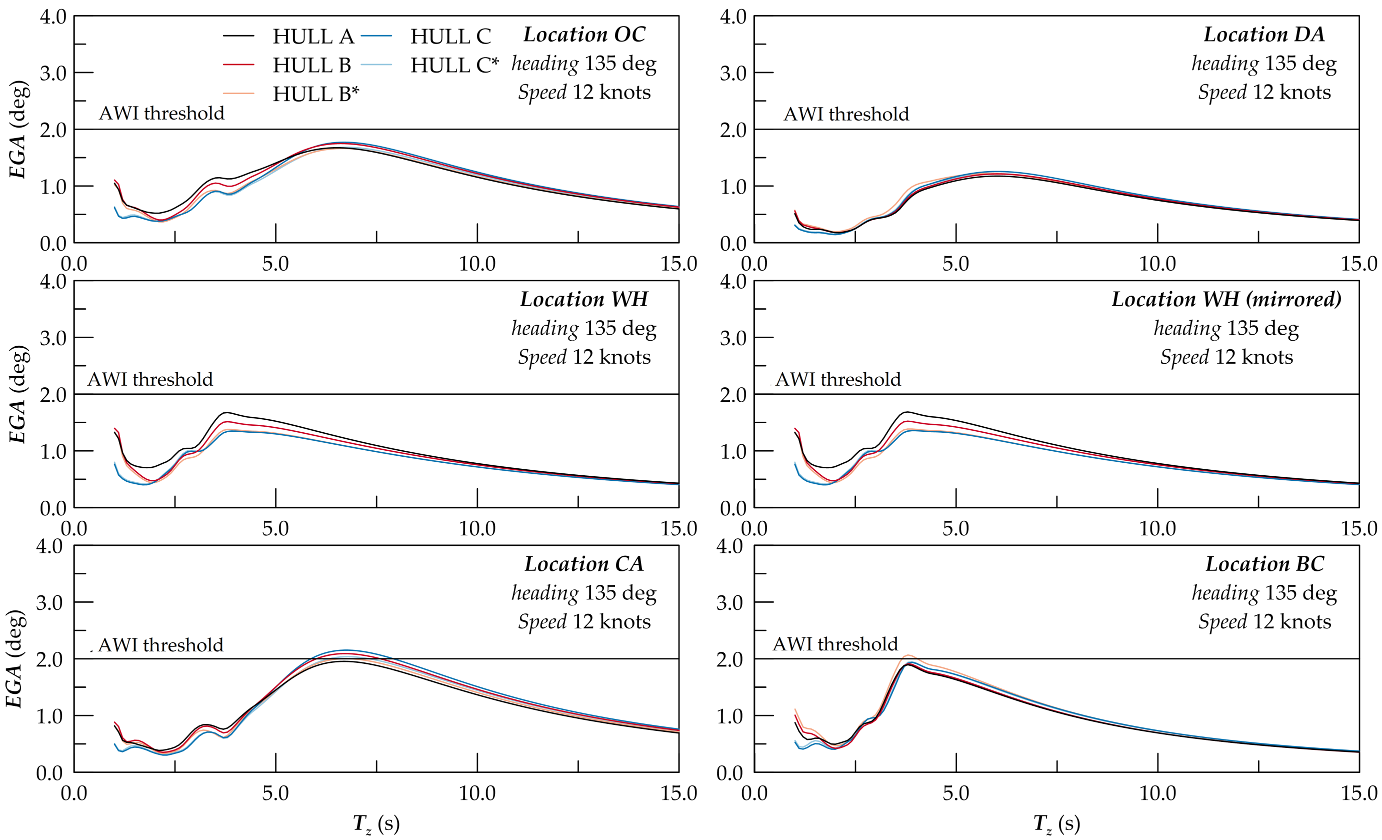

Figure 19. EGA values for $H_s = 1.5$ metres at different T_z for the AWI 22834 locations at 12 knots.

Figures 20 and 21 show the MSI values for the same conditions described for EGA calculations at the speeds of 0 and 12 knots, respectively. The thresholds visualised in the two figures correspond to a MSI value of 10% after 60 min of exposure, as suggested by AWI 22834 guidelines. Considering the zero speed condition (Figure 20), the threshold is exceeded by Hulls A, B and C for the wheel house (WH) location only. The other hulls do not exceed the MSI threshold at all. However, a speed increase is changing the critical conditions. At 12 knots (Figure 21), the dining area (DA) is the only location beyond the AWI threshold for MSI. All the other locations do not satisfy the given criterion for different ranges of T_z. For all the locations the hulls showing the best performances are C* and B*, with C* presenting the lower exceedance ranges for all locations.

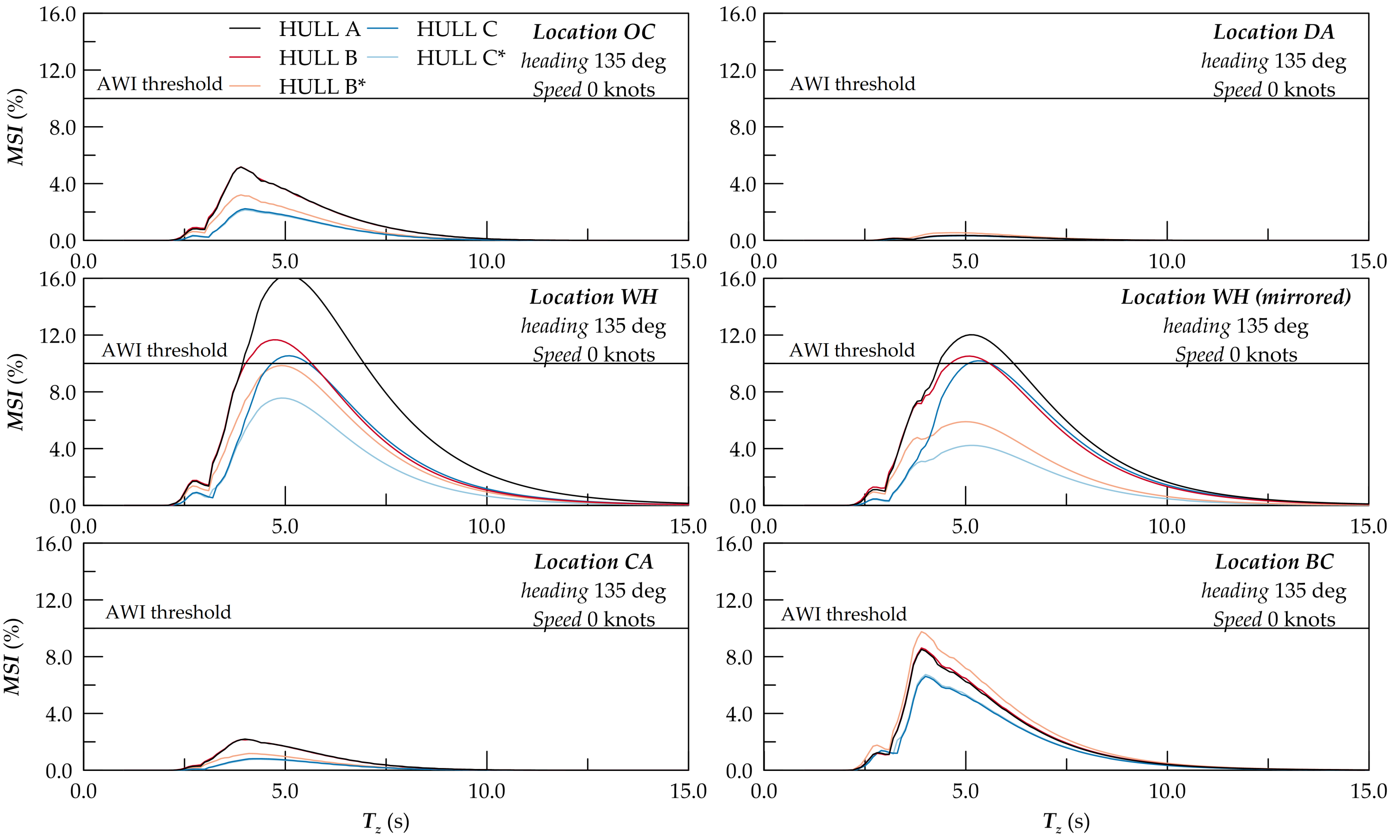

Figure 20. MSI values for $H_s = 1.5$ metres at different T_z for the AWI 22834 locations at 0 knots.

4.3. Comfort Rankings

With the availability of RMS values for EGA and MSI, it is possible to extract the downtime period of comfort fulfilment according to Equation (6). Table 5 reports the results, where only the AWI 22834 calculation points and conditions contribute to the final OP_C index. Besides OP_C, the rating is also shown through the AWI five-star scale, considering local and global comfort levels. The table reports for the WH location (the only one not on the diametral plain) the worst case between the original and mirrored positions on the x-axis.

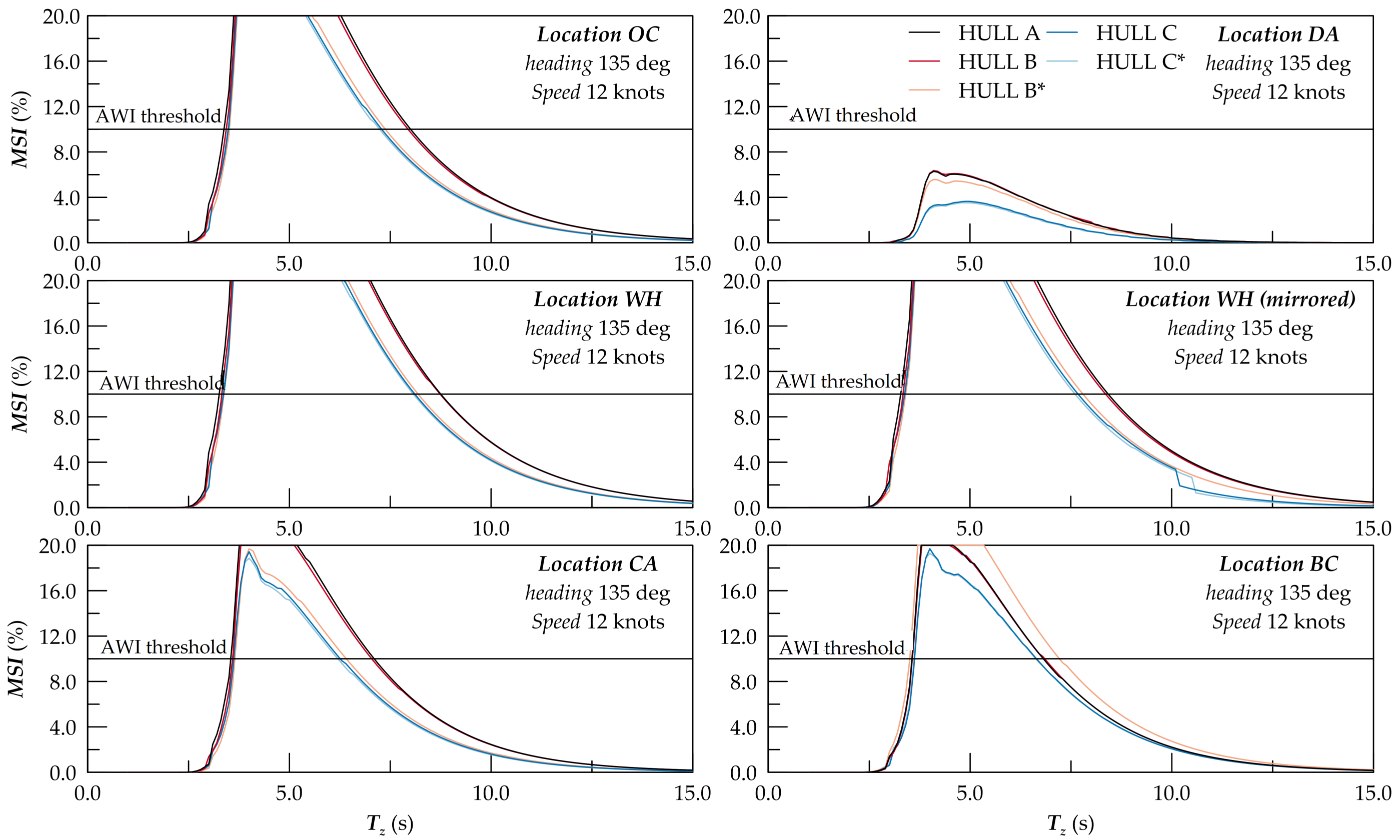

Figure 21. MSI values for $H_s = 1.5$ metres at different T_z for the AWI 22834 locations at 12 knots.

Table 5. OP_C and comfort ratings according to AWI 22834 criteria for the different hull concepts.

Location	HULL A		HULL B		HULL C		HULL B*		HULL C*	
	0 Knots	12 Knots	0 Knots	12 Knots	0 Knots	12 Knots	0 Knots	12 Knots	0 Knots	12 Knots
OC	2.26 ★☆☆☆☆	4.52 ★☆☆☆☆	2.26 ★☆☆☆☆	4.52 ★☆☆☆☆	2.26 ★☆☆☆☆	17.00 ★☆☆☆☆	2.26 ★☆☆☆☆	19.26 ★☆☆☆☆	2.39 ★☆☆☆☆	17.00 ★☆☆☆☆
DA	3.19 ★☆☆☆☆	100.00 ★★★★★	6.77 ★☆☆☆☆	100.00 ★★★★★	3.19 ★☆☆☆☆	100.00 ★★★★★	19.26 ★☆☆☆☆	100.00 ★★★★★	19.26 ★☆☆☆☆	100.00 ★★★★★
WH	19.25 ★☆☆☆☆	0.93 ★☆☆☆☆	47.41 ★★★☆☆	0.93 ★☆☆☆☆	65.07 ★★★★☆	4.52 ★☆☆☆☆	100.00 ★★★★★	4.52 ★☆☆☆☆	100.00 ★★★★★	4.52 ★☆☆☆☆
CA	2.26 ★☆☆☆☆	19.26 ★☆☆☆☆	2.26 ★☆☆☆☆	6.77 ★☆☆☆☆	2.26 ★☆☆☆☆	6.77 ★☆☆☆☆	2.26 ★☆☆☆☆	47.41 ★★★☆☆	2.26 ★☆☆☆☆	19.26 ★☆☆☆☆
BC	100.00 ★★★★★	19.26 ★☆☆☆☆	100.00 ★★★★★	19.26 ★☆☆☆☆	100.00 ★★★★★	19.26 ★☆☆☆☆	100.00 ★★★★★	19.26 ★☆☆☆☆	100.00 ★★★★★	19.26 ★☆☆☆☆
Partial	25.39 ★★☆☆☆	28.79 ★★☆☆☆	31.74 ★★☆☆☆	26.30 ★★☆☆☆	34.56 ★★☆☆☆	29.51 ★★☆☆☆	44.76 ★★★☆☆	38.09 ★★☆☆☆	44.78 ★★★☆☆	32.01 ★★☆☆☆
Total	27.09 ★★☆☆☆		29.02 ★★☆☆☆		32.04 ★★☆☆☆		41.43 ★★★☆☆		38.40 ★★☆☆☆	

The results allow a ranking to be established between the five different hull forms investigated in this study. Considering the final global OP_C as the principal classifier leads to the following scale:

1. **Hull B***: The solution with a conventional bulb and the same displacement of the initial hull results to be the solution with the highest OP_C for the AWI 22834 conditions. This solution scores high rankings for all the locations at both speeds, gaining the highest OP_C value for the crew area (CA) at 12 knots (47.41%). Even though the comfort characteristics are higher than for other solutions, the global ranking of the hull form remains average (3 stars out of five) according to the AWI 22834 scale.
2. **Hull C***: The vertical bow solution at the same displacement as the original yacht is the second-best design option according to the OP_C comfort rating. The main difference with Hull B* is for the crew area at 12 knots. Here, hull C* does not satisfy the EGA requirement for one scatter cell more than hull B*, leading to a local OP_C difference of about 18%. Comparing the OP_C at 0 knots, the C* solution provides the best comfort score. Applying the AWI 22834 scale, the hull form has comfort qualities below average (two stars out of five).
3. **Hull C**: The third-best ranking belongs to the vertical bow solution with the same draught as the original yacht. Compared to the original hull-form, the main differences concern all locations except the crew area (CA), where the performance of Hull A remains higher than Hull C for 12 knots. With an OP_C of 32%, the AWI scale remains the same as Hull C*, which means below average (two stars out of five).
4. **Hull B**: The rating of the conventional bow with a bulb is between the vertical bow solution and the original hull form by keeping the draught constant. Compared to the original hull, option B has better qualities at 0 knots but somewhat worse at 12 knots. With an OP_C of 29%, the AWI scale remains the same as Hull C, which means below average (two stars out of five).
5. **Hull A**: The worse comfort ranking is that of the original yacht, which means the conventional bow without a bulb. In any case, the AWI scale is the same as Hulls B, C and C*, which means comfort qualities are below average (two stars out of five).

The ranking provided by applying AWI 22834 comfort criteria favours design solution B* with a conventional bow with a bulb at the same displacement as the original yachts (Hull A). However, the ranking is specific to the analysed case and influenced by environmental condition granularity and locations used for this reference yacht. The main difference between Hulls B* and C* concerns the crew area at the speed of 12 knots, where the satisfaction of the EGA criterion for a single cell increases the local OP_C by 18%. As the global score between C* and B* is close, and Hull C has a higher ranking than Hull B, it could be supposed that the best solution for comfort may be the vertical bow. Such an assumption implies adopting a different granularity for the environmental conditions or alternative locations, or the execution of more complex seakeeping analyses or simulations. Considering comfort analyses on the combined scatter diagram of Areas 26 and 47 confirms the possible advantages of a vertical bow. Figures 22 and 23 report the limiting curves for the comfort criteria on all AWI locations. The limiting envelopes highlight that for the combined set of H_s–T_z couples, Hull C* exceeds the comfort thresholds for lower cells compared to other hull forms. Such a consideration is valid at both 0 and 12 knots. The observed trend on the combined scatter diagram is not in line with the conventional AWI 22834 environmental conditions.

It is then necessary to discuss further possible developments and integrations to the present study aiming at a more reliable definition of design guidelines for large yachts.

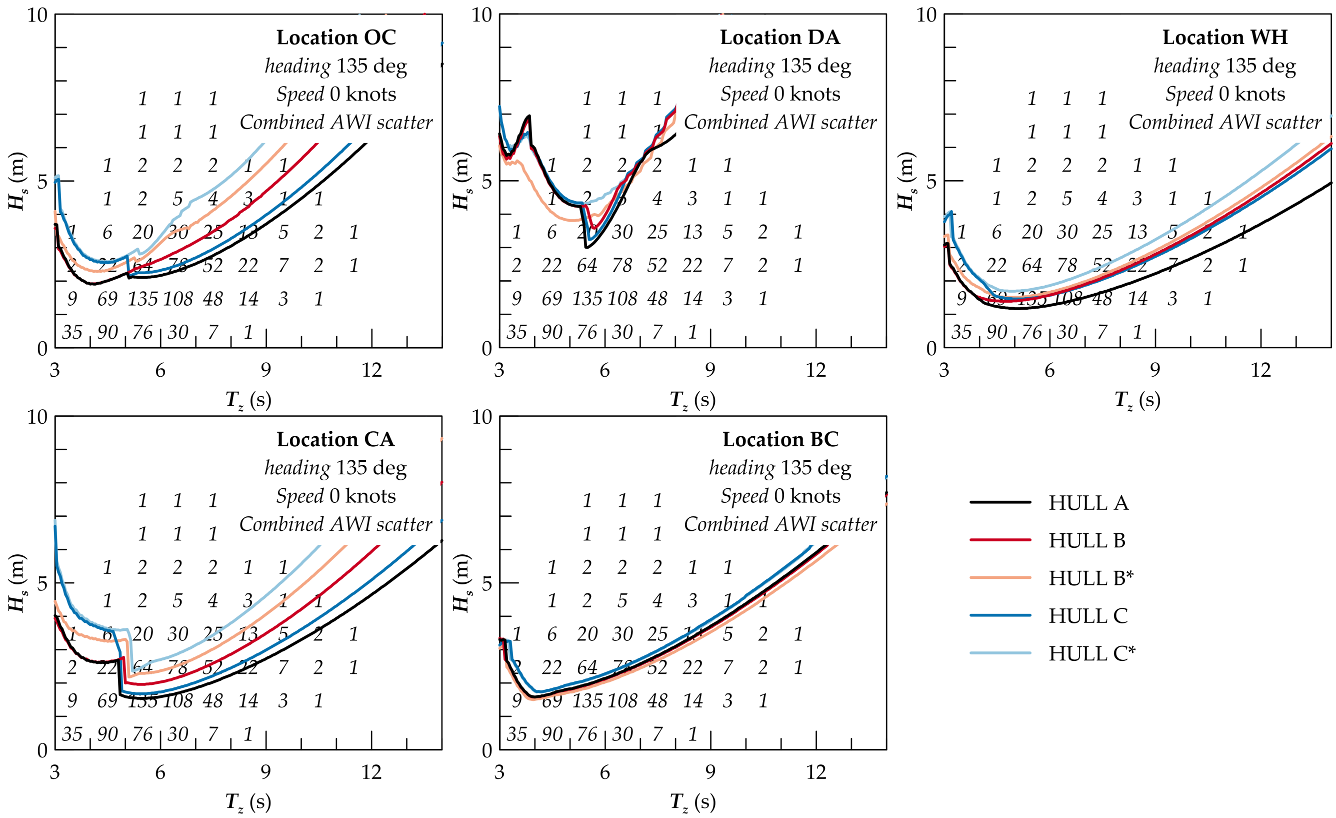

Figure 22. Limiting comfort criteria curves on the combined Area 27 and 47 scatter diagram for the AWI 22834 locations at 0 knots.

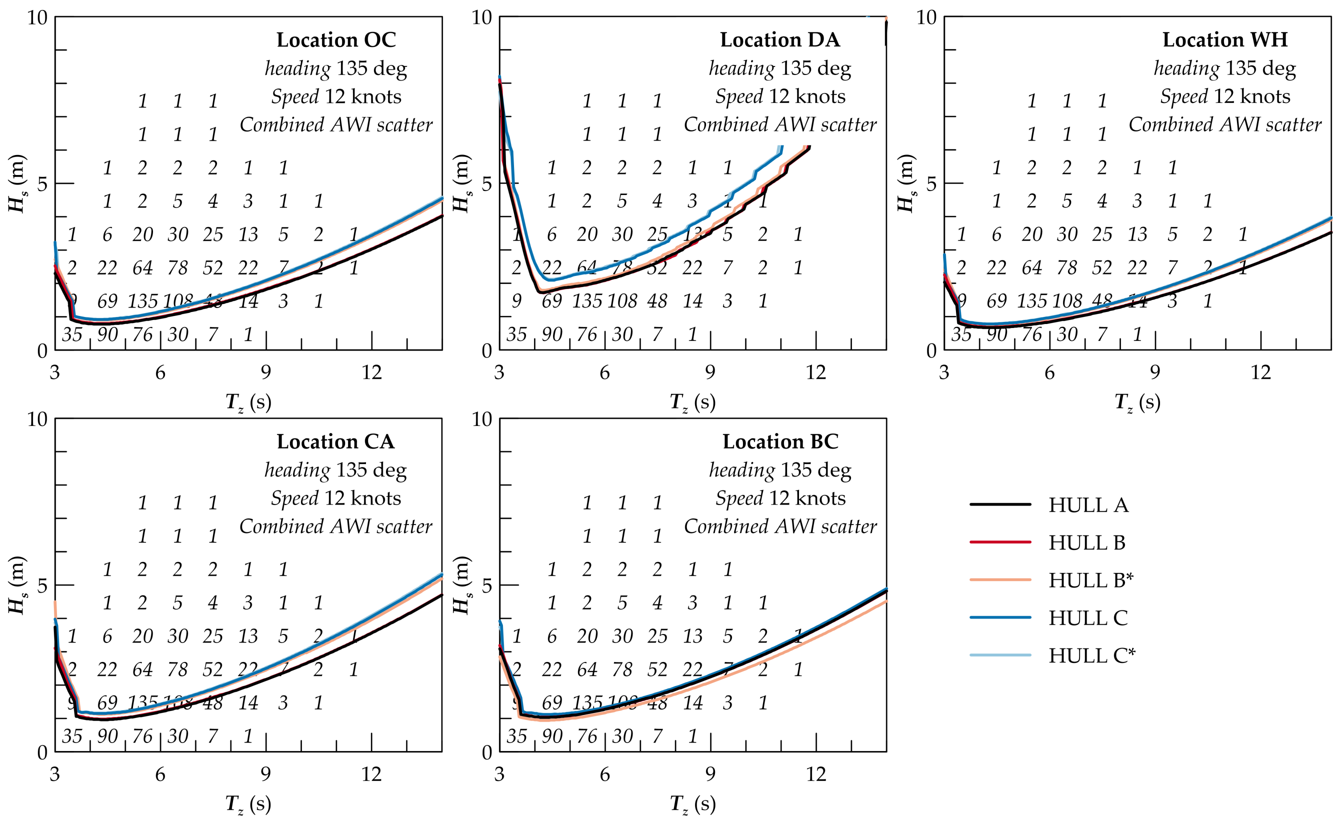

Figure 23. Limiting comfort criteria curves on the combined Area 27 and 47 scatter diagram for the AWI 22834 locations at 12 knots.

5. Discussion

The comfort analysis performed according to the AWI 22834 guidelines established a ranking between the five analysed bow design solutions for the reference large yacht. The results highlighted a somewhat unexpected trend, giving the best rank to hull B* fitted with a conventional bow and a nested bulb.

However, a more in-depth seakeeping analysis on a broader range of environmental conditions shows a preference for hull C*, representing the vertical bow concept. Such a result, obtained by applying the same comfort criteria of AWI guidelines and the same numerical models of the main study reported in this work, suggests that AWI 22834 guidelines are not a suitable metric to derive design indications for large yachts. The consideration is valid at least once the comfort analysis employs strip-theory calculations. Furthermore, the ranking includes only comfort criteria, not the only design attribute for a large yacht, especially once green [41,42] and digital [43] transitions are becoming extremely relevant to the ship design process.

Therefore, the following main areas require a focus for further improvement of present comfort analysis and the determination of general guidelines on hull form concepts for designers:

- Comfort criteria and environmental conditions.
- Numerical analysis of seakeeping characteristics.
- Inclusion of additional parameters not related only to comfort (resistance, added resistance, manoeuvering, etc.).

A way forward to include the mentioned points on design guidelines of large yachts requires a preliminary discussion in the following sections.

5.1. Identification of More Reliable Comfort Criteria

The results of the comfort calculations presented in the previous section highlight an inconsistency with the expectations of the best form for designing a large yacht bow. The investigation of a broader set of environmental conditions shows how the vertical bow is maybe the best solution for motion reduction. Furthermore, considering different definitions of the JONSWAP spectrum can also be a source of changes in the global ranking according to AWI guidelines.

Table 6 reports the differences in OP_C values obtained by changing the definition of the elongation parameter γ. Keeping $\gamma = 1.0$ invariant with T_z (which means considering a set of Pierson–Moskowitz spectra) does not change the ranking between the bow solutions. The OP_C values are close to the original analysis referring to a variable γ. The spectrum modification influences only one condition of the AWI environmental definition, more precisely, the one corresponding to $T_z = 3.5$ s. On the other hand, an invariant $\gamma = 3.3$ changes the final ranking among the hulls. The γ value corresponding to 3.3 is the standard parameter suggested to model a not fully developed irregular sea state in the North Sea; however, designers use it as a constant reference value for sea areas. The elongation parameter modifies the peak shape of the spectra (see Figure 17 for $T_z = 3.5$ s), thus the coupling between the wave spectrum and RAO. Consequently, the final values of OP_C change the original rankings, showing higher comfort levels than $\gamma = 1$ or variable γ cases. OP_C increases from 5 to 7% for all the hull forms except for Hull B*, where the value remains almost constant. Then, the best solution becomes Hull C*, thus the vertical bow concept.

Furthermore, the AWI 22834 guidelines suggest $\chi = 135$ degrees as the reference for comfort analysis. Previous studies [13,44] show that such an assumption is arguable, as certain yachts may result in worse motions for other headings. At the same time, MSI and EGA adoption as key parameter indicators requires accurate revision, as it is influenced by the vessel dimensions, compromising the generality of the ranking process. In conclusion, despite the purpose of the AWI 22834 guidelines being the establishment of general criteria to rank the performances of different yachts, such standards need to be further investigated to develop an instrument suitable to derive hull form design guidelines for large yachts.

Table 6. OP_C and comfort ratings according to different γ definitions for JONSWAP spectra.

γ (-)	HULL A	HULL B	HULL C	HULL B*	HULL C*
variable	27.09 ★★☆☆☆	29.09 ★★☆☆☆	32.04 ★★☆☆☆	41.43 ★★★☆☆	38.40 ★★☆☆☆
$\gamma = 3.3$	34.68 ★★☆☆☆	35.94 ★★☆☆☆	36.45 ★★☆☆☆	41.55 ★★★☆☆	45.35 ★★★☆☆
$\gamma = 1.0$	26.86 ★★☆☆☆	29.02 ★★☆☆☆	32.03 ★★☆☆☆	40.97 ★★★☆☆	38.39 ★★☆☆☆

5.2. Numerical Assumptions and Non-Linear Effects

The present study uses a 2D strip-theory method to solve the numerical problem of ship motion. As already explained, the purpose was to employ a methodology of easy access and comprehension for designers at an early design stage. However, with the constant increase of computational power potentially at disposal in design offices, more accurate 3D panel methods allow for preliminary motion assessment as well. Three-dimensional panel codes have the advantage of including the radiation problem more, leading to a different definition of forces than 2D strip-theory codes. Furthermore, the discretisation of the hull form with panels instead of sections could better capture the differences between hull forms, especially in the case of slight variations. It is, therefore, handy to study whether the adoption of such computation techniques gives an improvement or not to comfort evaluation.

Nevertheless, a frequency domain 3D panel code represents a linear resolution of ship motions. The motion equations give rise to a linear response if all the coefficients are independent of the motion amplitude. In principle, this requires that the variations of the wetted surface during the vessel oscillation are negligible, so the relative motion amplitudes must be small enough. Although the amplitudes of ship motions are large, the submerged part of the hull can vary considerably, and the linear approximation is not valid any more. Roll is generally the motion that is more influenced by nonlinearities, especially when the damping is small. Non-linear effects are relevant for large-amplitude oscillations that rarely occur for the environmental conditions proposed by AWI guidelines. However, non-linear effects can be significant when phenomena associated with slamming are analysed, thus comfort associated with high-frequency hull vibrations. It is then necessary also to analyse these phenomena in dedicated studies.

5.3. Multi-Criteria Analysis of Hull Form Solutions

The present study focuses on comfort only and is principally associated with ship motion analysis in irregular waves. However, the design of a large yacht or a ship, in general, requires evaluating multiple attributes [45]. These are concurrently contributing to the overall performance of the vessel [46]. For example, the addition of a skeg may influence the yacht's performances in manoeuvring, seakeeping and resistance [47], or the bow shape can be beneficial for motion behaviour and not in propulsion.

Including multicriterial processes in the hull form design also requires a deep understanding of the yacht's operative profile and the necessities of the shipowner. The performance attributes influencing the hull form design may lead to opposite solutions, the intrinsic necessities of motion and resistance reduction being antithetical. In a design process nowadays oriented to green transition, the benefit given by a decrease in consumption/emission could be more effective than a slight OC_C variation for comfort. It is, therefore, necessary to identify with dedicated studies the relative importance of different design parameters and their impact on the yacht's performance. Only providing a global weighted overview of the advantages and disadvantages of alternative hull solutions allows general and functional guidelines for designers to be determined.

6. Conclusions

The present work presents a comfort analysis on a large yacht based on the AWI 22834 guidelines to investigate the effect of different bow shapes on the motion behaviour of the vessel in irregular waves. Five hull forms describe the most adopted bow design solutions in the yachting market, analysing constant draught or displacement hulls.

The comfort analysis determined a ranking between the different hull forms, indicating the conventional bow solution with the nested bulb as the design option granting higher comfort for the AWI 22834 locations, service and environmental conditions. Such a hull form (Hull B*) has a comfort rate OP_C just 3% higher than the vertical bow solution at the same displacement (Hull C*), only due to the behaviour in a single location (the crew area) at the speed of 12 knots. Nevertheless, this difference determines a ranking variation between the two forms according to the AWI 22834 star rating system, from below average (two out of five stars) to good (three out of five stars). The execution of comfort analysis on a broader set of Hs–Tz couples highlights that the effective exceedance of AWI comfort limits is lower for vertical bow hulls.

Such a consideration, together with results published for yachts of different sizes [13,44], suggests that the AWI 22834 guidelines are not the appropriate metrics to properly assess comfort levels on large yachts and satisfactorily compare hull form design solutions. The discussion of the obtained results on the reference yacht allows the further steps needed for defining versatile design guidelines for large yachts to be determined with more insight, especially for the early design stage. As such, the present study lacks a proper definition of inertia which can be crucial in further changing the final comfort level in different design solutions. However, a better inclusion of such an effect requires the availability of real yacht building data to establish a proper statistical formulation of inertia values for different yacht types. As mentioned, the present study focuses on the pure effect of the bow form on the seakeeping characteristics of a yacht, without aiming at the definition of an optimal hull form. The results show that the differences of comfort level due to the bow shape only are not significant, suggesting that better comfort levels may be reached by changing other global hull parameters not touched in this study. Nonetheless, the effect of the bow change may be more relevant to other yacht's performances such as resistance.

Further studies on a broader cluster of dimensions and forms are necessary for identifying more general metrics for comfort ranking and for defining reliable environmental and encounter conditions. Furthermore, the influence on comfort ratings of adopting more advanced calculation techniques should be checked and compared with strip theory, including non-linear effects, if the case. Lastly, the analysis must include other design parameters, such as fuel consumption and emissions, which are crucial for a large yacht or, generally, for a ship.

Nevertheless, the present study is a good starting point for identifying design guidelines for a future generation of large yachts, which, besides comfort, will face the challenges given by the imminent ecological and digital transitions in the shipping industry and ship design.

Author Contributions: Conceptualization, F.M. and E.D.V.; methodology, F.M.; software, F.M.; validation, E.D.V., F.M. and R.N.; formal analysis, F.M. and E.D.V.; investigation, E.D.V. and F.M.; data curation, F.M.; writing—original draft preparation, F.M.; writing—review and editing, B.R., E.B., E.D.V. and F.M.; visualization, F.M. and B.R.; supervision, E.B. and R.N. All authors have read and agreed to the published version of the manuscript.

Funding: This research received no external funding.

Institutional Review Board Statement: Not applicable.

Informed Consent Statement: Not applicable.

Data Availability Statement: Not applicable.

Conflicts of Interest: The authors declare no conflict of interest.

Abbreviations

The following abbreviations are used in this manuscript:

AWI	Approved work item
BC	Beach club
CA	Crew area
CR	Comfort rating
DA	Dining area
DOF	Degree of freedom
EGA	Effective gravity angle
ISO	International Organization for Standardization
JONSWAP	Joint North Sea Wave Project
MARIN	Maritime Research Institute of the Netherlands
MIR	Motion Illness Rating
MSI	Motion Sickness Index
OC	Owner's cabin
RAO	Response amplitude operator
RMS	Root mean square
WH	Wheel house

References

1. McCauly, M.E.; Royal, J.W.; Wylie, C.D.; O'Hanlon, J.F.; Mackie, R. *Motion Sickness Incidence: Exploratory Studies of Habituation, Pitch and Roll, and the Refinement of a Mathematical Model*; Technical report; Canyon Research Group Inc.: Goleta, CA, USA, 1976.
2. Wieringen, H.V.; Gumbs, F.; Dallinga, R.; Bos, J. Practical Experience on Reducing Motions and Improving Comfort on Board Large Motor Yachts. In Proceedings of the 16th International Symposium on Yacht Design and Yacht Construction, HISWA, Amsterdam, The Netherlands, 2000.
3. TNO. *TNO-DV 2007 C232*; Technical report; TNO: Delft, Netherlands, 2007.
4. Lawther, A.; Griffin, M. Motion sickness and motion characteristics of vessels at sea. *Ergonomics* **1988**, *31*, 1373–1394. [CrossRef] [PubMed]
5. Islam, R.; Abbassi, R.; Garaniya, V.; Kahn, F. Development of a human reliability assessment technique for the maintenance procedures of marine and offshore operations. *J. Loss Prev. Process. Ind.* **2017**, *50*, 416–428. [CrossRef]
6. Islam, R.; Khan, F.; Abbassi, R.; Garaniya, V. Human Error Probability Assessment During Maintenance Activities of Marine Systems. *Saf. Health Work.* **2018**, *9*, 42–52. [CrossRef] [PubMed]
7. Bittner, A.; Guignard, J. Human Factors Engineering Principles for Minimizing Adverse Ship Motion Effects: Theory and Practice. *Nav. Eng. J.* **1985**, *97*, 205–213. [CrossRef]
8. Endrina, N.; Konovessis, D.; Sourina, O.; Krishnan, G. Influence of ship design and operational factors on human performance and evaluation of effects and sensitivity using risk models. *Ocean. Eng.* **2019**, *184*, 143–158. [CrossRef]
9. Bittner, A.; Guignard, J. Shipboard evaluation of motion sickness incidence and human engineering problems. *J. Low Freq. Noise Vib.* **1988**, *7*, 50–65. [CrossRef]
10. Mitkov, T.; Dovramadjiev, D. Investigation of the Luxury Yachts Condition and their Maintenance. *Int. J. Eng. Manag. Sci.* **2022**, *7*, 95–105.
11. Graham, R. Motion Induced Interruptions as Ship Operability Criteria. *Nav. Enginners J.* **1990**, *102*, 65–71. [CrossRef]
12. Backer, C.; Sweeney, K. Setting a standard for luxury and comfort. In Proceedings of the Design, Construction and Operation of Super and Mega Yachts Conference, Genova, Italy, 1–2 April 2009.
13. Mauro, F.; Benci, A.; Ferrari, V.; Della Valentina, E. Dynamic positioning analysis and comfort assessment for the early design stage of large yachts. *Int. Shipbuild. Prog.* **2021**, *68*, 33–60. [CrossRef]
14. Della Valentina, E. *ISO/AWI 22834 Large Yachts–Quality Assessment of Life on-Board*; Technical report; MARIN: Wageningen, The Netherlands, 2019.
15. Muntjewerf, J.J. The influence of shipform and length on the behaviour of destroyer-type ships in head and beam seas. *Int. Shipbuild. Prog.* **1963**, *10*, 37–52. [CrossRef]
16. Grigoropoulos, G.; Chalkias, D. Hull-form optimization in calm and rough water. *CAD Comput. Aided Des.* **2010**, *42*, 977–984. [CrossRef]
17. Gammon, M. Optimization of fishing vessels using a Multi-Objective Genetic Algorithm. *Ocean. Eng.* **2011**, *38*, 1054–1064. [CrossRef]
18. Scamardella, A.; Piscopo, V. Passenger ship seakeeping optimization by the Overall Motion Sickness Incidence. *Ocean. Eng.* **2014**, *76*, 86–97. [CrossRef]
19. Vernengo, G.; Brizzolara, S.; Bruzzone, D. Resistance and seakeeping optimization of a fast multihull passenger ferry. *Int. J. Offshore Polar Eng.* **2015**, *25*, 26–34.

20. Nazemian, A.; Ghadimi, P. Multi-objective optimization of trimaran sidehull arrangement via surrogate-based approach for reducing resistance and improving the seakeeping performance. *Proc. Inst. Mech. Eng. Part M J. Eng. Marit. Environ.* **2021**, *235*, 944–956. [CrossRef]
21. Renaud, P.; Sacher, M.; Scolan, Y.M. Multi-objective hull form optimization of a SWATH configuration using surrogate models. *Ocean. Eng.* **2022**, *256*, 111209. [CrossRef]
22. Liu, S.; Papanikolaou, A.; Zaraphonitis, G. Prediction of added resistance of ships in waves. *Ocean. Eng.* **2011**, *38*, 641–650. [CrossRef]
23. Liu, S.; Papanikolaou, A. Regression analysis of experimental data for added resistance in waves of arbitrary heading and development of a semi-empirical formula. *Ocean. Eng.* **2020**, *206*, 107357. [CrossRef]
24. Loukakis, T.; Chryssostomidis, C. Seakeeping standard series for cruiser-stern ships. *Trans. Soc. Nav. Archit. Mar. Eng.* **1975**, *3*, 15.
25. Mauro, F.; Dell'Acqua, A. Vertical motions assessment of an offshore supply vessel in concept design stage. In Proceedings of the Technology and Science for the Ships of the Future—Proceedings of NAV 2018: 19th International Conference on Ship and Maritime Research, Trieste, Italy, 20–22 June 2018.
26. Gerritsma, J.; Beukelman, W. The influence of a bulbous bow on the motions and the propulsion in longitudinal waves. *Int. Shipbuild. Prog.* **1963**, *10*, 149–158. [CrossRef]
27. NORDFORSK. *Assessment of Ship Performance in a Seaway*; Technical report; NORDFORSK: Oslo, Norway, 1987.
28. NATO. *STANAG 4154 Common Procedures for Seakeeping in the Ship Design Process*; Technical report; NATO: Brussels, Belgium, 2000.
29. Grin, R.; van Heerd, J.; Ferrari, V. Hydrodynamic aspects in the design of passenger vessels. In Proceedings of the RINA, Royal Institution of Naval Architects—Design and Operation of Passenger Ships, London, UK, 20–21 November 2013.
30. Mauro, F.; Prpić-Oršić, J. Determination of a DP operability index for an offshore vessel in early design stage. *Ocean. Eng.* **2020**, *195*, 106764. [CrossRef]
31. Kracht, A. Design of bulbous bows. *SNAME Trans.* **1978**, *86*, 197–217.
32. Holtrop, J.; Mennen, G. An approximate power prediction method. *Int. Shipbuild. Prog.* **1982**, *335*, 166–170. [CrossRef]
33. Sharma, R.; Sha, O. Practical Hydrodynamic Design of Bulbous Bows for Ships. *Nav. Eng. J.* **2008**, *1*, 57–76. [CrossRef]
34. Della Valentina, E. *70040.102 Effect of Bow Flare on Rigid Body Accelerations for Displacement Motor Yacht*; Technical report; MARIN: Wageningen, The Netherlands, 2014.
35. Determining a Vessel's Load Line Length. Available online: https://dco.uscg.mil/LLLength (accessed on 22 December 2022).
36. SHIPMO Fast Seakeeping Calculations: Behaviour of a Ship in a Seaway. Available online: https://https://www.marin.nl/en/facilities-and-tools/software (accessed on 23 December 2022).
37. Ikeda, Y. On roll damping force of ship-effect of friction of hull and normal force of bilge keels. *J. Soc. Nav. Archit. Jpn.* **1976**, *161*.
38. van Daalen, E. Numerical and Theoretical Studies of Water Waves and Floating Bodies. Ph.D. Thesis, University of Twente, Enschede, The Netherlands, 1993.
39. DNV. *DNV RP C205 Environmental Conditions and Environmental Loads*; Technical report; Det Norske Veritas: Hovik, Norway, 2014.
40. Mauro, F.; Vassalos, D. An area-specific survivability assessment for passenger ships. In Proceedings of the SNAME 14th International Marine Design Conference, IMDC 2022, Vancouver, BC, Canada, 26–30 June 2022.
41. Mauro, F.; Ghigliossi, E.; Bucci, V.; Marinó, A. Design of hybrid-electric megayachts: The impact of operative profile and smart berthing infrastructures. *J. Mar. Sci. Eng.* **2021**, *9*, 1–18. [CrossRef]
42. Begovic, E.; Bertorello, C.; De Luca, F.; Rinauro, B. KISS (Keep It Sustainable and Smart): A Research and Development Program for a Zero-Emission Small Crafts. *J. Mar. Sci. Eng.* **2022**, *10*, 16. [CrossRef]
43. Mauro, F.; Kana, A. Digital twin for ship life-cycle: A critical systematic review. *Ocean. Eng.* **2023**, *269*, 113479. [CrossRef]
44. Mauro, F.; Benci, A.; Ferrari, V.; Della Valentina, E. Dynamic Positioning analysis for the early-design stage of large yachts. In Proceedings of the 26th HISWA Symposium on Yacht Design and Constructions, 2020.
45. Papanikolaou, A. *Ship Design: Methodologies of Preliminary Design*; Springer: Berlin/Heidelberg, Germany, 2014.
46. Papanikolaou, A.; Harries, S.; Hooijmans, P.; Marzi, J.; Nena, R.; Torben, S.; Yrjan, A.; Boden, B. A Holistic Approach to Ship Design: Tools and Applications. *J. Ship Res.* **2022**, *66*, 25–63. [CrossRef]
47. Ferrari, V.; Gornicz, T.; Kisjes, A.; Quadvlieg, F.H. Influence of skeg on ship manoeuvrability at high and low speeds. In Proceedings of the 14th International Symposium on Practical Design of Ships and other Floating Structures PRADS 2019, Yokohama, Japan, 22–26 September 2019.